Possible existing seismic analysis errors of long span structures and bridges while utilizing multi-point earthquake calculation models

Wei Guo, Zhi-wu Yu, Guo-huan Liu & Zhen Guo

Bulletin of Earthquake Engineering
Official Publication of the European Association for Earthquake Engineering

ISSN 1570-761X

Bull Earthquake Eng
DOI 10.1007/s10518-013-9462-3

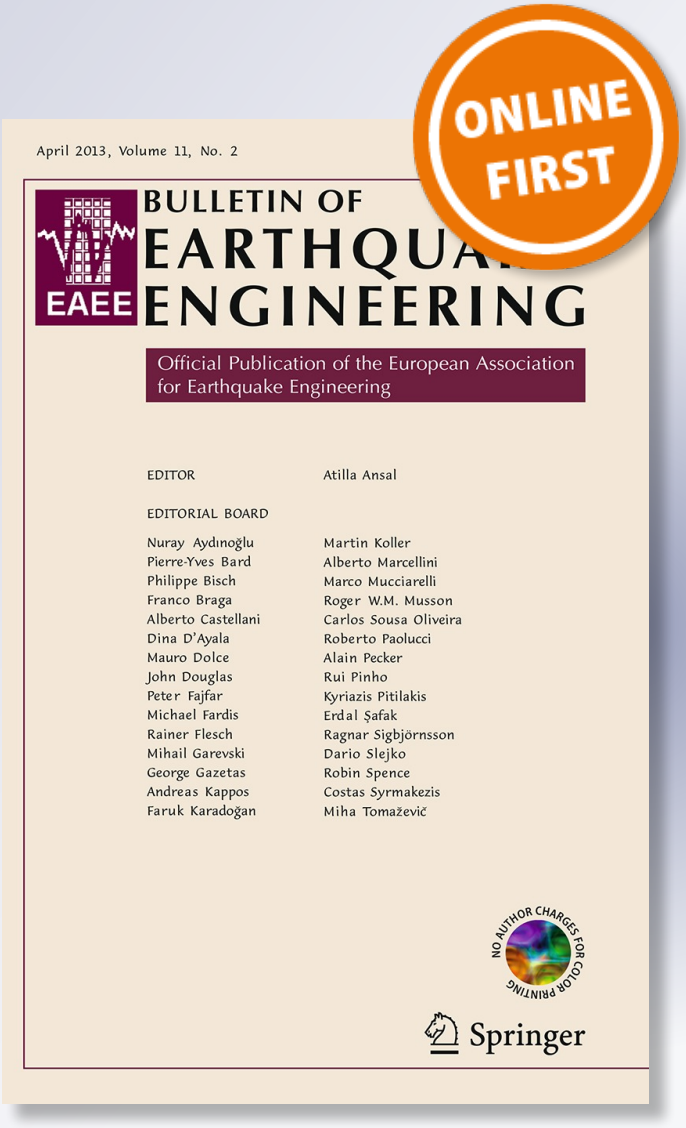

Springer

Bull Earthquake Eng
DOI 10.1007/s10518-013-9462-3

ORIGINAL RESEARCH PAPER

Possible existing seismic analysis errors of long span structures and bridges while utilizing multi-point earthquake calculation models

Wei Guo · Zhi-wu Yu · Guo-huan Liu · Zhen Guo

Received: 1 December 2012 / Accepted: 5 May 2013

Abstract A long-span structure is a common type of public building, but its seismic characteristics are distinct from other types of buildings because of its long span. Calculation models considering multi-point excitation are required in the seismic analysis of long-span structures. However, correlative studies have already clearly shown that important but often overlooked errors exist in previously developed multi-point excitation calculation models. The process of establishing displacement and acceleration models for multi-point seismic analysis is reviewed. Error sources and criteria of the two models are explained using rigorous theoretical derivation. Error characteristics and distributions in multiple structural types, such as ordinary structures without dampers and damper-installed structures with concentrated damping, are also described. Modifications for multi-point excitation displacement and acceleration models, for time history and stochastic analysis, respectively, are proposed, and these modified models are used to assess errors in the conventional models. Numerical examples are solved using conventional displacement and acceleration models and two corresponding modified models. The properties, components and distribution of errors in the conventional models are demonstrated. The findings presented in this paper can provide a sound basis for the practical application of multi-point excitation calculation models in seismic analysis.

Keywords Long-span structure · Seismic analysis · Multi-point excitation · Calculation model · Damping problem

W. Guo (✉) · Z. Yu
National Engineering Laboratory for High Speed Railway Construction, School of Civil Engineering, Central South University, Changsha 410075, China
e-mail: wei.guo.86@gmail.com

G. Liu
School of Civil and Hydraulic Engineering, Tsinghua University, Beijing 100084, China

Z. Guo
Department of Civil Engineering, Zhejiang University, Hangzhou 310027, China

Published online: 16 May 2013

1 Introduction

Social progress and economic development in recent years have stimulated the growth of the public-sector construction industry around the world and especially in China. Numerous buildings with complex structural styles have been constructed in China, such as the "Bird's Nest" National Stadium, the World Expo Theme Pavilion in Shanghai, high-speed railway stations and others. All of these large structures possess long-span characteristics and often are landmarks of a city. Long-span structures play a role in transportation structures. Urbanization and urban population growth have increased transportation demand and vehicle traffic. A large number of interurban elevated bridges are to be constructed to meet these needs. High-speed railway lines, a large proportion of which are often bridges, are being built as well. Because of their important functions and symbolic significance, seismic analysis and design of long-span structures and bridges have attracted widespread attention from scholars. The seismic response characteristics of long-span structures are clearly distinct from ordinary structures, especially when the structural span's wavelength and the ground's wavelength are the same order of magnitude. Differences between multiple earthquake excitations applied to supports should be considered, mainly in connection with the following three important factors: wave passage effects, local site effects and site coherence effects. In general, calculated results ignoring multi-point excitation characteristics cannot accurately describe actual structural response.

Seismic analysis of long-span structures under multi-point excitation has become a focus of current research. Two calculation models are usually adopted, the displacement model and the acceleration model. The displacement model takes the displacement of the ground in an earthquake as its input and uses the absolute structural displacement as a key parameter. This model has a wide range of application and is suitable for both linear and nonlinear analysis. Using the displacement model, Yamamura and Tanaka (1990), Hao (1991), Hao and Xiao (1995), Su et al. (2006) have carried out a great deal of numerical work on time history analysis of engineering structures. The acceleration model takes the acceleration of the ground in an earthquake as its input. This model was first proposed by Clough and Penzien (1975) based on rigorous theoretical derivation. It is similar in form to the model that is established under uniform seismic excitation. The acceleration model has good accuracy but is only suitable for linear analysis because of the superposition principle adopted in its derivation. However, this point is often overlooked in application, and applying the acceleration model to nonlinear analysis of long-span structures leads to incorrect results and unreasonable designs. Acceleration response spectrum methods suitable for seismic analysis of long-span structures have been derived by Kiureghian and Ansgar (1992) and Berrah and Kausel (1993). Given that both the displacement model and the acceleration model have certain inherent assumptions associated with them, they possess some theoretical defects and are not applicable for all conditions. Considering that few scholars have studied the error-inducing aspects of these models, we identified problem of the displacement model in ordinary structures with Rayleigh damping and showed that the problem can be addressed by the use of a massless rigid element (MRE) in the SAP2000 software (Liu et al. 2010). However, in the previous study, only ordinary structures with Rayleigh damping were considered. As the styles of long-span structures are usually diverse and conventional designs cannot satisfy practical seismic needs, control techniques, such as isolation, dampers and so on, are often introduced in design. Therefore, long-span structures with isolation or dampers that possess concentrated damping characteristics appear frequently in engineering. Considering that the reliability and error potential of conventional seismic calculation models have not been addressed before, the study described in this paper is considered valuable and timely.

Based on research previously conducted by we, two calculation models (the displacement model and the acceleration model) for seismic analysis of long-span structures subjected to multi-point excitation are systematically studied, focusing in particular on their applicability and error potential for ordinary structures and damper-installed structures that possess concentrated damping characteristics. First, sources of error and situations in which they may arise are analyzed for the two models by rigorous theoretical derivation. It is demonstrated that the error problem is mainly the result of a non-proportional damping distribution. Second, modifications to the displacement and acceleration models, for time history and stochastic analysis, respectively, are presented. Third, numerical analyses are presented to demonstrate the error magnitudes and distributions of the two models for different types of structures. The effectiveness of the proposed model modifications is also verified. The results of the study described in this paper provide important guidance for the rational use and modification of calculation models for seismic analysis of long-span structures under multi-point excitation in earthquakes.

2 Calculation models for seismic analysis under multi-point excitation

As part of this study of the errors in calculation models for seismic analysis of long-span structures under multi-point excitation, rigorous theoretical derivations of the displacement model and the acceleration model are conducted to clarify their basic assumptions and corresponding approximations adopted in the derivation process.

2.1 Displacement model

In an earthquake, ground motion will cause motion in a structure, and due to its own inertia, the structure will experience deformation. Figure 2 gives a diagrammatic sketch of long-span structure with multiple supports on ground. As shown in Fig. 2, all of the degrees of freedom (DOFs) of the structural system can be divided into the following two parts: non-constrained DOFs (referred to as non-constrained parts or upper parts) and constrained DOFs (referred to as constrained parts or lower parts), which can be . Taking absolute displacements as the key parameters, the dynamic equilibrium equation of the structural system as a whole can be established as follows:

$$\begin{bmatrix} \boldsymbol{M}_s & \boldsymbol{M}_{sb} \\ \boldsymbol{M}_{\mathrm{bs}} & \boldsymbol{M}_b \end{bmatrix} \begin{Bmatrix} \ddot{\boldsymbol{U}}_s \\ \ddot{\boldsymbol{U}}_b \end{Bmatrix} + \begin{bmatrix} \boldsymbol{C}_s & \boldsymbol{C}_{sb} \\ \boldsymbol{C}_{\mathrm{bs}} & \boldsymbol{C}_b \end{bmatrix} \begin{Bmatrix} \dot{\boldsymbol{U}}_s \\ \dot{\boldsymbol{U}}_b \end{Bmatrix} + \begin{bmatrix} \boldsymbol{K}_s & \boldsymbol{K}_{sb} \\ \boldsymbol{K}_{\mathrm{bs}} & \boldsymbol{K}_b \end{bmatrix} \begin{Bmatrix} \boldsymbol{U}_s \\ \boldsymbol{U}_b \end{Bmatrix} = \begin{Bmatrix} \boldsymbol{0} \\ R_b \end{Bmatrix} \tag{1}$$

in which M_s, $\boldsymbol{C}_s$ and K_s are respectively mass, damping and stiffness matrices of the upper parts of the structure. M_b, $\boldsymbol{C}_b$ and K_b are matrices of the lower parts of the structure. $M_{bs} = M_{sb}^T$, $\boldsymbol{C}_{bs} = \boldsymbol{C}_{sb}^T$ and $K_{bs} = K_{sb}^T$ correspond to coupling mass, damping and stiffness matrices between the upper and lower parts. R_b is a force acting on supports provided by the foundation. $\boldsymbol{U}_s$, $\dot{\boldsymbol{U}}_s$ and $\ddot{\boldsymbol{U}}_s$ are absolute displacement, velocity and acceleration vectors of the upper parts of the structure. Similarly, $\boldsymbol{U}_b$, $\dot{\boldsymbol{U}}_b$ and $\ddot{\boldsymbol{U}}_b$ correspond to absolute displacement, velocity and acceleration of the supports. Because supports will move together with the ground in an earthquake, these vectors actually describe ground motion. In general, the dynamic equilibrium equation for a structure in an earthquake is established in Eq. (1) by absolute movement, which is correct in theory and has been mentioned in several references (Wilson 2004). What needs to be explained is that stiffness and damping force are both described by absolute displacement, which apparently is in contrast with its usual expression by relative displacement. In view of the characteristics of the stiffness matrix, equivalent

increases of all displacements will not influence the stiffness force. This point also applies to damping characteristics that come from structural stiffness or dampers. Meanwhile, mass damping, as a part of the damping matrix, is proportional to the mass matrix, which only possesses diagonal elements, so force provided by mass damping and produced by absolute displacement in Eq. (1) is in theory different from that produced by relative displacement. This means that different results will be obtained depending on whether absolute or relative displacement is adopted to establish a calculation model. However, the force provided by mass damping is usually small and has little effect on the calculated results and the damping mechanism in an actual project is complex and hard to confirm. Therefore, Eq. (1) approximately equals the equation given by relative displacement. According to the above description, the dynamic equilibrium equation of upper parts of the structure can be given by Eq. (2):

$$\boldsymbol{M}_{\mathrm{s}}\ddot{\boldsymbol{U}}_s + \boldsymbol{C}_{\mathrm{s}}\dot{\boldsymbol{U}}_s + \boldsymbol{K}_{\mathrm{s}}\boldsymbol{U}_s = -\boldsymbol{M}_{\mathrm{sb}}\ddot{\boldsymbol{U}}_b - \boldsymbol{C}_{\mathrm{sb}}\dot{\boldsymbol{U}}_b - \boldsymbol{K}_{\mathrm{sb}}\boldsymbol{U}_{\mathrm{b}} \tag{2}$$

If lumped mass is adopted here, $\boldsymbol{M}_{\mathrm{sb}} = 0$, the above equation can be rewritten as:

$$\boldsymbol{M}_{\mathrm{s}}\ddot{\boldsymbol{U}}_s + \boldsymbol{C}_{\mathrm{s}}\dot{\boldsymbol{U}}_s + \boldsymbol{K}_{\mathrm{s}}\boldsymbol{U}_s = -\boldsymbol{C}_{\mathrm{sb}}\dot{\boldsymbol{U}}_{\mathrm{b}} - \boldsymbol{K}_{\mathrm{sb}}\boldsymbol{U}_{\mathrm{b}} \tag{3}$$

The usual practice is to ignore the damping force $-\boldsymbol{C}_{\mathrm{sb}}\dot{\boldsymbol{U}}_{\mathrm{b}}$ because the magnitude of the damping force is difficult to define precisely. This practice is reasonable for ordinary structures with the lower parts not excessively elementally divided. The following equation can be given:

$$\boldsymbol{M}_{\mathrm{s}}\ddot{\boldsymbol{U}}_s + \boldsymbol{C}_{\mathrm{s}}\dot{\boldsymbol{U}}_s + \boldsymbol{K}_{\mathrm{s}}\boldsymbol{U}_s = -\boldsymbol{K}_{\mathrm{sb}}\boldsymbol{U}_{\mathrm{b}} \tag{4}$$

in which $\boldsymbol{U}_{\mathrm{b}}$ represents absolute displacement of the ground in an earthquake. $-\boldsymbol{K}_{\mathrm{sb}}\boldsymbol{U}_{\mathrm{b}}$ is the concentrated force applied on the upper parts of the structure by supports. Equation (4) is known as the displacement model and it requires absolute displacement time histories as input. The displacement model is a widely applicable model that is suitable not only for uniform excitation but also for multi-point non-uniform excitation. Moreover, as there are no assumptions adopted in its derivation, this model can be used for both linear and nonlinear analysis. However, as described in the derivation, Eq. (4) is obtained by ignoring the damping force $-\boldsymbol{C}_{\mathrm{sb}}\dot{\boldsymbol{U}}_{\mathrm{b}}$ and this approximation may lead to some problems in seismic analysis of long-span structures. In general, the problem can be described as follows: when the lower parts of an ordinary structure are excessively elementally divided, the stiffness of structural elements near supports is great, and thus, the displacement model will produce erroneous results. This problem was identified by we in a previous study and a solution developed using the SAP2000 software was proposed and numerically verified (Liu et al. 2010). Thus, Eq. (3) can be considered an accurate calculation model for seismic analysis of long-span structures, and Eq. (4) (the displacement model) is an approximate model ignoring parts of the damping force, which may cause obvious errors in some situations. This result is confirmed by numerical analyses later in this paper.

2.2 Acceleration model

The acceleration model is established by transformation of Eq. (3) and requires acceleration time histories of ground motion in an earthquake. The usual practice is to divide absolute displacements of the structure into two parts:

$$\boldsymbol{U}_s = \boldsymbol{U}_s^d + \boldsymbol{U}_s^p = \boldsymbol{U}_s^d + \boldsymbol{\Gamma}_{sb}\boldsymbol{U}_b \tag{5}$$

in which $\boldsymbol{U}_s^d$ is usually referred to as the dynamic displacement and $\boldsymbol{U}_s^p$ as the quasi-static displacement. $\boldsymbol{\Gamma}_{sb}$ is the transformation matrix. $\boldsymbol{U}_b$ is the ground displacement in an earthquake.

Matrix $\boldsymbol{\Gamma}_{sb}$ can be set to an arbitrary value so that different combinations of structural response can be constructed to correspond to different solution strategies (Su et al. 2006). However, $\boldsymbol{\Gamma}_{sb}$ is usually given by eliminating the inertia force and damping force in Eq. (4), which yields the following expression:

$$\boldsymbol{K}_s\boldsymbol{\Gamma}_{sb}\boldsymbol{U}_b = -\boldsymbol{K}_{sb}\boldsymbol{U}_b \Rightarrow \ \boldsymbol{\Gamma}_{sb} = -\boldsymbol{K}_s^{-1}\boldsymbol{K}_{sb} \tag{6}$$

Substituting Eqs. (5) and (6) into Eq. (3), it can be rewritten as:

$$\boldsymbol{M}_{\mathrm{s}}\ddot{\boldsymbol{U}}_s^d + \boldsymbol{C}_{\mathrm{s}}\dot{\boldsymbol{U}}_s^d + \boldsymbol{K}_{\mathrm{s}}\boldsymbol{U}_s^d = -\boldsymbol{M}_{\mathrm{s}}\boldsymbol{\Gamma}_{sb}\ddot{\boldsymbol{U}}_b - (\boldsymbol{C}_{\mathrm{sb}} + \boldsymbol{C}_{\mathrm{s}}\boldsymbol{\Gamma}_{sb})\,\dot{\boldsymbol{U}}_{\mathrm{b}} - (\boldsymbol{K}_{\mathrm{sb}} + \boldsymbol{K}_{\mathrm{s}}\boldsymbol{\Gamma}_{sb})\,\boldsymbol{U}_{\mathrm{b}} \tag{7}$$

Obviously, $\boldsymbol{K}_{\mathrm{sb}} + \boldsymbol{K}_{\mathrm{s}}\boldsymbol{\Gamma}_{sb} = \boldsymbol{K}_{\mathrm{sb}} - \boldsymbol{K}_{\mathrm{s}}\boldsymbol{K}_s^{-1}\boldsymbol{K}_{sb} = 0$, so the third term to the right of the equal sign can be eliminated. Moreover, if only stiffness damping is assumed for the whole structure, the second term can also be eliminated: $-(\boldsymbol{C}_{\mathrm{sb}} + \boldsymbol{C}_{\mathrm{s}}\boldsymbol{\Gamma}_{sb})\,\dot{\boldsymbol{U}}_{\mathrm{b}} = -\beta\,(\boldsymbol{K}_{\mathrm{sb}} + \boldsymbol{K}_{\mathrm{s}}\boldsymbol{\Gamma}_{sb})\,\dot{\boldsymbol{U}}_{\mathrm{b}} = 0$.

If the damping characteristics of the structure include not only stiffness damping but also mass damping, the damping term $-(\boldsymbol{C}_{\mathrm{sb}} + \boldsymbol{C}_{\mathrm{s}}\boldsymbol{\Gamma}_{sb})\,\dot{\boldsymbol{U}}_{\mathrm{b}}$ actually does not equal zero exactly. Nonetheless, this term can also be ignored in calculation because $-(\boldsymbol{C}_{\mathrm{sb}} + \boldsymbol{C}_{\mathrm{s}}\boldsymbol{\Gamma}_{sb})\,\dot{\boldsymbol{U}}_{\mathrm{b}}$ in an ordinary structure is usually small and because $-(\boldsymbol{C}_{\mathrm{sb}} + \boldsymbol{C}_{\mathrm{s}}\boldsymbol{\Gamma}_{sb})\,\dot{\boldsymbol{U}}_{\mathrm{b}}$ is hard to define accurately in practical applications. Thus, the following expression is given:

$$\boldsymbol{M}_{\mathrm{s}}\ddot{\boldsymbol{U}}_s^d + \boldsymbol{C}_{\mathrm{s}}\dot{\boldsymbol{U}}_s^d + \boldsymbol{K}_{\mathrm{s}}\boldsymbol{U}_s^d = \boldsymbol{M}_{\mathrm{s}}\boldsymbol{K}_s^{-1}\boldsymbol{K}_{sb}\ddot{\boldsymbol{U}}_b \tag{8}$$

in which $\boldsymbol{\Gamma}_{sb} = -\boldsymbol{K}_s^{-1}\boldsymbol{K}_{sb}$. Equation (8) is usually referred to as the acceleration model for seismic analysis of long-span structures. The acceleration model cannot be used in nonlinear analysis because its derivation depends on adoption of the superposition principle. Particularly when the ground motion is uniform earthquake excitation, this means that $\ddot{\boldsymbol{U}}_b = \boldsymbol{E}\ddot{u}_g$, $\boldsymbol{E} = [1, 1, \ldots, 1]^T$, in which $\ddot{u}_g$ is ground acceleration. $\boldsymbol{\Gamma}_{sb} = \boldsymbol{I}$ is usually adopted instead of $\boldsymbol{\Gamma}_{sb} = -\boldsymbol{K}_s^{-1}\boldsymbol{K}_{sb}$. An acceleration model applicable for uniform earthquake excitation can be written as:

$$\boldsymbol{M}_{\mathrm{s}}\ddot{\boldsymbol{U}}_s^d + \boldsymbol{C}_{\mathrm{s}}\dot{\boldsymbol{U}}_s^d + \boldsymbol{K}_{\mathrm{s}}\boldsymbol{U}_s^d = -\boldsymbol{M}_{\mathrm{s}}\boldsymbol{E}\ddot{u}_g \tag{9}$$

This is the calculation model used most often in seismic analysis of structures. It is established based only on relative displacement. As shown in the above derivation, the acceleration model of Eq. (8) is an approximate model, similar to the displacement model, because it ignores the damping term $-(\boldsymbol{C}_{\mathrm{sb}} + \boldsymbol{C}_{\mathrm{s}}\boldsymbol{\Gamma}_{sb})\,\dot{\boldsymbol{U}}_{\mathrm{b}}$. The accuracy of this model is limited by this approximation. The damping term is small enough to be neglected in seismic response calculation for ordinary structures. However, in structures possessing concentrated damping characteristics (non-proportional damping), such as isolated structures and damper-installed structures, this ignored damping term will lead to obvious errors in calculation.

Because both of the displacement model and acceleration model are derived by relying on approximations that are not valid for all situations, the two models have some potential for error and are limited in their respective scopes of application. The research work in this paper is conducted to investigate the two models' error sources and situations in which errors may occur and to propose corresponding modifications to achieve satisfactory calculation precision.

3 Error in the calculation model

When dealing with long-span structures under multi-point earthquake excitation, the error magnitude is usually determined by the ignored damping term if the model used adopts

the approximation of ignoring damping. This point applies to both the displacement model and the acceleration model, so the error problem actually can be considered the damping problem. The following section examines the damping problem in these two models and the corresponding errors that result when are applied to several different types of structures. To analyze the error situations of calculation models accurately, all structural modes should be considered and the damping matrix should be established using the same strategy. These steps are taken to avoid the influence of irrelevant factors in the study.

3.1 Displacement model

Regardless of what assumption is made concerning damping in the structure, the ignored damping term $-\boldsymbol{C}_{\mathrm{sb}}\dot{\boldsymbol{U}}_{\mathrm{b}}$ is always a source of error in the displacement model. For example, when Rayleigh damping and lumped mass are adopted, the following expression can be given:

$$-\boldsymbol{C}_{\mathrm{sb}}\dot{\boldsymbol{U}}_{\mathrm{b}} = -\left(\alpha\boldsymbol{M}_{\mathrm{sb}} + \beta\boldsymbol{K}_{\mathrm{sb}}\right)\dot{\boldsymbol{U}}_{\mathrm{b}} = -\beta\boldsymbol{K}_{\mathrm{sb}}\dot{\boldsymbol{U}}_{\mathrm{b}} \tag{10}$$

Considering the way in which matrix $\boldsymbol{K}_{\mathrm{sb}}$is constructed, it can be observed that the ignored damping force is directly proportional to the stiffness of bottom elements connected to the supports. However, the stiffness force in the displacement model increases with $\boldsymbol{K}_{\mathrm{sb}}$, so the error magnitude of the displacement model is difficult to evaluate using Eq. (10) only. To evaluate the error of the displacement model, the following expression can be obtained from Eqs. (4) and (5):

$$\boldsymbol{M}_{\mathrm{s}}\ddot{\boldsymbol{U}}_s^d + \boldsymbol{C}_{\mathrm{s}}\dot{\boldsymbol{U}}_s^d + \boldsymbol{K}_{\mathrm{s}}\boldsymbol{U}_s^d = -\boldsymbol{M}_{\mathrm{s}}\boldsymbol{\Gamma}_{sb}\ddot{\boldsymbol{U}}_b - \boldsymbol{C}_{\mathrm{s}}\boldsymbol{\Gamma}_{sb}\dot{\boldsymbol{U}}_b - \left(\boldsymbol{K}_{\mathrm{sb}} + \boldsymbol{K}_{\mathrm{s}}\boldsymbol{\Gamma}_{sb}\right)\boldsymbol{U}_b \tag{11a}$$

$$\boldsymbol{U}_s = \boldsymbol{U}_s^d + \boldsymbol{U}_s^p = \boldsymbol{U}_s^d + \boldsymbol{\Gamma}_{sb}\boldsymbol{U}_b = \boldsymbol{U}_s^d - \boldsymbol{K}_{\mathrm{s}}\boldsymbol{K}_s^{-1}\boldsymbol{U}_b \tag{11b}$$

Because of transformation equivalence, results obtained from Eq. (11) equal those from the displacement model and Eq. (11a) can be used to calculate the structural response $\boldsymbol{U}_s^d$. Given that $\boldsymbol{K}_{\mathrm{sb}} + \boldsymbol{K}_{\mathrm{s}}\boldsymbol{\Gamma}_{sb} = \boldsymbol{K}_{\mathrm{sb}} - \boldsymbol{K}_{\mathrm{s}}\boldsymbol{K}_s^{-1}\boldsymbol{K}_{sb} = 0$, Eq. (11) can be converted to:

$$\boldsymbol{M}_{\mathrm{s}}\ddot{\boldsymbol{U}}_s^d + \boldsymbol{C}_{\mathrm{s}}\dot{\boldsymbol{U}}_s^d + \boldsymbol{K}_{\mathrm{s}}\boldsymbol{U}_s^d = -\boldsymbol{M}_{\mathrm{s}}\boldsymbol{\Gamma}_{sb}\ddot{\boldsymbol{U}}_b - \boldsymbol{C}_{\mathrm{s}}\boldsymbol{\Gamma}_{sb}\dot{\boldsymbol{U}}_b \tag{12a}$$

$$\boldsymbol{U}_s = \boldsymbol{U}_s^d + \boldsymbol{U}_s^p = \boldsymbol{U}_s^d + \boldsymbol{\Gamma}_{sb}\boldsymbol{U}_b = \boldsymbol{U}_s^d - \boldsymbol{K}_{\mathrm{s}}\boldsymbol{K}_s^{-1}\boldsymbol{U}_b \tag{12b}$$

Equation (12) is derived from the displacement model and is obviously similar to the acceleration model, except that Eq. (12a) contains an additional damping term $-\boldsymbol{C}_{\mathrm{s}}\boldsymbol{\Gamma}_{sb}\dot{\boldsymbol{U}}_b$. Here, the acceleration model can be considered as an accurate model for an ordinary structure, as explained subsequently. Equation (12) is used to evaluate the error of the displacement model. If Rayleigh damping is adopted for an ordinary structure, the damping term $-\boldsymbol{C}_{\mathrm{s}}\boldsymbol{\Gamma}_{sb}\dot{\boldsymbol{U}}_b$ can be expressed as

$$-\boldsymbol{C}_{\mathrm{s}}\boldsymbol{\Gamma}_{sb}\dot{\boldsymbol{U}}_b = -\left(\alpha\boldsymbol{M}_s + \beta\boldsymbol{K}_s\right)\boldsymbol{\Gamma}_{sb}\dot{\boldsymbol{U}}_b = -\alpha\boldsymbol{M}_s\boldsymbol{\Gamma}_{sb}\dot{\boldsymbol{U}}_b - \beta\boldsymbol{K}_{sb}\dot{\boldsymbol{U}}_b \tag{13}$$

in which α and β are respectively proportional coefficients of mass damping and stiffness damping that can be calculated by modal frequencies and corresponding damping ratios. Substituting Eq. (13) into Eq. (12a):

$$\boldsymbol{M}_{\mathrm{s}}\ddot{\boldsymbol{U}}_s^d + \boldsymbol{C}_{\mathrm{s}}\dot{\boldsymbol{U}}_s^d + \boldsymbol{K}_{\mathrm{s}}\boldsymbol{U}_s^d = -\boldsymbol{M}_{\mathrm{s}}\boldsymbol{\Gamma}_{sb}\ddot{\boldsymbol{U}}_b - \alpha\boldsymbol{M}_s\boldsymbol{\Gamma}_{sb}\dot{\boldsymbol{U}}_b - \beta\boldsymbol{K}_{sb}\dot{\boldsymbol{U}}_b \tag{14}$$

Based on the superposition principle within the linear range, the structural response $\boldsymbol{U}_s^d$ consists of three components, $\boldsymbol{U}_{s,1}^d$, $\boldsymbol{U}_{s,2}^d$ and $\boldsymbol{U}_{s,3}^d$, which are produced by forces

$-\boldsymbol{M}_s\boldsymbol{\Gamma}_{sb}\ddot{\boldsymbol{U}}_b$, $-\alpha\boldsymbol{M}_s\boldsymbol{\Gamma}_{sb}\dot{\boldsymbol{U}}$ and $-\beta\boldsymbol{K}_{sb}\dot{\boldsymbol{U}}_b$, respectively. To describe the relative magnitudes of the three components conveniently, the following parameters are given:

$$\kappa_{21} = \frac{\left\|-\alpha\boldsymbol{M}_s\boldsymbol{\Gamma}_{sb}\dot{\boldsymbol{U}}\right\|_\infty}{\left\|-\boldsymbol{M}_s\boldsymbol{\Gamma}_{sb}\ddot{\boldsymbol{U}}_b\right\|_\infty} \approx |\alpha|\,\frac{\|\boldsymbol{M}_s\boldsymbol{\Gamma}_{sb}\|_\infty\left\|\dot{\boldsymbol{U}}\right\|_\infty}{\|\boldsymbol{M}_s\boldsymbol{\Gamma}_{sb}\|_\infty\left\|\ddot{\boldsymbol{U}}_b\right\|_\infty} = |\alpha|\,\frac{\left\|\dot{\boldsymbol{U}}\right\|_\infty}{\left\|\ddot{\boldsymbol{U}}_b\right\|_\infty} \tag{15a}$$

$$\kappa_{31} = \frac{\left\|-\beta\boldsymbol{K}_{sb}\dot{\boldsymbol{U}}_b\right\|_\infty}{\left\|-\boldsymbol{M}_s\boldsymbol{\Gamma}_{sb}\ddot{\boldsymbol{U}}_b\right\|_\infty} \approx |\beta|\,\frac{\|\boldsymbol{K}_{sb}\|_\infty}{\|\boldsymbol{M}_s\|_\infty\|\boldsymbol{\Gamma}_{sb}\|_\infty}\,\frac{\left\|\dot{\boldsymbol{U}}\right\|_\infty}{\left\|\ddot{\boldsymbol{U}}_b\right\|_\infty} \approx |\beta|\,\frac{\|\boldsymbol{K}_{sb}\|_\infty}{\|\boldsymbol{M}_s\|_\infty}\,\frac{\left\|\dot{\boldsymbol{U}}\right\|_\infty}{\left\|\ddot{\boldsymbol{U}}_b\right\|_\infty} \tag{15b}$$

in which κ_{21} describes the magnitude of $-\alpha\boldsymbol{M}_s\boldsymbol{\Gamma}_{sb}\dot{\boldsymbol{U}}$ relative to $-\boldsymbol{M}_s\boldsymbol{\Gamma}_{sb}\ddot{\boldsymbol{U}}_b$, and κ_{31} describes magnitude of $-\beta\boldsymbol{K}_{sb}\dot{\boldsymbol{U}}_b$ relative to $-\boldsymbol{M}_s\boldsymbol{\Gamma}_{sb}\ddot{\boldsymbol{U}}_b$. A simple and approximate calculation is performed using maximum values in Eq. (15). In Eq. (15a), because $|\alpha| < 1$ and velocity is generally smaller than acceleration, κ_{21} must be a small value. Acceleration in an earthquake is actually a dynamic input to the structure and velocity can be treated as a static load because of its long period. Thus, the response produced by load $-\boldsymbol{M}_s\boldsymbol{\Gamma}_{sb}\ddot{\boldsymbol{U}}_b$ has an amplification compared with static loading and the approximate response produced by load $-\alpha\boldsymbol{M}_s\boldsymbol{\Gamma}_{sb}\dot{\boldsymbol{U}}$ has no amplification. In general, $\boldsymbol{U}^d_{s,2}$ produced by the second term on the right side of Eq. (14) can be ignored in comparison with $\boldsymbol{U}^d_{s,1}$. In Eq. (15b), $|\beta| < 1$ and velocity is also smaller than acceleration, but the stiffness term is larger than the mass term. Given that $\boldsymbol{K}_{sb}$ contains only the stiffness of bottom elements, it is reasonable to describe $\|\boldsymbol{M}_s\|_\infty$ in Eq. (15b) by the mass of bottom elements. When the bottom of the structure is too finely elementally divided, $\boldsymbol{M}_s$ corresponding to the mass of bottom elements will be very small and $\boldsymbol{K}_{sb}$ corresponding to the stiffness of bottom elements will be very large, so κ_{21} will also be a large value. This means that the third term on the right side of Eq. (14) cannot be ignored in comparison with the first term. Thus, the calculated results tend to diverge from the correct solution obtained with better elemental division of the structural bottom. In general, in ordinary structures with Rayleigh damping assumption, the error problem of the displacement model can be qualitatively explained as follows: if bottom elements are normally divided, results from the displacement model are sufficiently accurate. However, if bottom elements are too finely divided, adopting the displacement model for seismic analysis leads to some obvious error in the calculated results and the magnitude of this error is significantly related to the bottom elemental division.

An approximate error evaluation index for the displacement model is described as follows. According to Eq. (15b) the error is mainly produced by $-\beta\boldsymbol{K}_{sb}\dot{\boldsymbol{U}}_b$, which has a non-zero value only at the bottom of the structure. Defining the stiffness matrix of bottom elements as k_{sb} and earthquake acceleration of corresponding supports as $\dot{u}_b$, the magnitudes of the non-zero items in $-\beta\boldsymbol{K}_{sb}\dot{\boldsymbol{U}}_b$ can be described by $|\beta k_{sb}\dot{u}_b|$, and the magnitudes of the items in $-\boldsymbol{M}_s\boldsymbol{\Gamma}_{sb}\ddot{\boldsymbol{U}}_b$ corresponding to bottom elements are approximately equal to $|m_s\ddot{u}_b|$. Acceleration in an earthquake is a dynamic input to the structure, so compared with static loading there is an amplification effect. The velocity input can be considered a static load on the structure because of its long period. In China's seismic code, the dynamic magnification factor is assumed to be 2.25. Using this value, the ratio of responses produced by $-\beta\boldsymbol{K}_{sb}\dot{\boldsymbol{U}}_b$ to those produced by $-\boldsymbol{M}_s\boldsymbol{\Gamma}_{sb}\ddot{\boldsymbol{U}}_b$ is written as:

$$\tau = (|\beta|/2.25)\,(k_{sb}/m_{s1})\,(\mathrm{PGV}/\mathrm{PGA}) \tag{16}$$

in which PGV is the maximum value of ground velocity and PGA is the maximum value of ground acceleration in an earthquake. $\tau/(1+\tau)$ is approximately equal to the error of the displacement model and can be used to evaluate error situations.

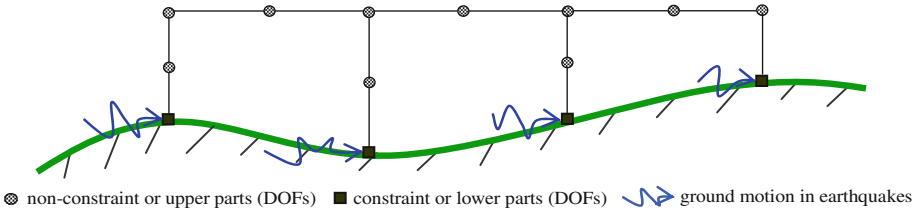

Fig. 1 Schematic diagram of long-span structure model

When dampers are installed to control the seismic response of a structure, concentrated damping exists in addition to Rayleigh damping, so in this situation the structure possesses non-proportional damping characteristics, and is usually referred to as a non-proportionally damped structure. Even if the structural elements are not too finely divided, the ignored $-\boldsymbol{C}_{\mathrm{sb}}\dot{\boldsymbol{U}}_{\mathrm{b}}$ in the displacement model includes concentrated damping that exists in the connection between the supports and upper parts of structure, so the model precision will also be influenced. However, the displacement model can produce accurate results when concentrated damping exists in internal parts of the structure. Here, internal parts of structure mean nodes and elements of the non-constraint parts in Fig. 1, and excluding elements between non-constraint and constraint DOFs.

Considering that the stiffness provided by additional dampers has no effect on model precision, if we assume that the damping matrix provided by dampers in the connection between the supports and the upper parts of structure is $\boldsymbol{C}_{\mathrm{d1}}$, the ignored damping term $-\boldsymbol{C}_{\mathrm{sb}}\dot{\boldsymbol{U}}_{\mathrm{b}}$ in the displacement model can be expressed as

$$-\boldsymbol{C}_{\mathrm{sb}}\dot{\boldsymbol{U}}_{\mathrm{b}} = -\beta\boldsymbol{K}_{\mathrm{sb}}\dot{\boldsymbol{U}}_{\mathrm{b}} - \boldsymbol{C}_{d1}\dot{\boldsymbol{U}}_{\mathrm{b}} \tag{17}$$

Thus, the error of the displacement model is influenced by both stiffness damping and concentrated damping. Therefore, except in the case of too fine an elemental division of the structural bottom, base isolation with concentrated damping at the bottom of the structure will also lead to some error in the displacement model. Referring to Eq. (16), the error index involving the influence of element division and concentrated damping can be expressed as follows:

$$\tau = (|\beta|/2.25)\,[(k_{sb} + c_d/\beta)/m_{s1}]\,(\mathrm{PGV}/\mathrm{PGA}) \tag{18}$$

3.2 Acceleration model

In the acceleration model, one usually adopts a static transformation matrix $\boldsymbol{\Gamma}_{sb} = -\boldsymbol{K}_s^{-1}\boldsymbol{K}_{sb}$ to decompose the structural response, and $-(\boldsymbol{C}_{\mathrm{sb}} + \boldsymbol{C}_{\mathrm{s}}\boldsymbol{\Gamma}_{sb})\,\dot{\boldsymbol{U}}_{\mathrm{b}}$ is the source of error in the acceleration model. When Rayleigh damping and lumped mass are assumed in structure, $\boldsymbol{C}_{\mathrm{sb}} = \beta\boldsymbol{K}_{sb}$, $\boldsymbol{C}_{\mathrm{s}} = \alpha\boldsymbol{M}_s + \beta\boldsymbol{K}_s$, the following expression is obtained:

$$-(\boldsymbol{C}_{\mathrm{sb}} + \boldsymbol{C}_{\mathrm{s}}\boldsymbol{\Gamma}_{sb})\,\dot{\boldsymbol{U}}_{\mathrm{b}} = -[\beta\boldsymbol{K}_{\mathrm{sb}} + (\alpha\boldsymbol{M}_{\mathrm{s}} + \beta\boldsymbol{K}_{\mathrm{s}})\,\boldsymbol{\Gamma}_{sb}]\,\dot{\boldsymbol{U}}_{\mathrm{b}} = \alpha\boldsymbol{M}_{\mathrm{s}}\boldsymbol{\Gamma}_{sb}\dot{\boldsymbol{U}}_{\mathrm{b}} \tag{19}$$

The damping term $\beta\boldsymbol{K}_{\mathrm{sb}}\dot{\boldsymbol{U}}_{\mathrm{b}}$ related to structural stiffness has been eliminated in calculation, so the error magnitude is mainly determined by mass damping, which is $\alpha\boldsymbol{M}_{\mathrm{s}}\boldsymbol{\Gamma}_{sb}\dot{\boldsymbol{U}}_{\mathrm{b}} = \alpha\boldsymbol{M}_{\mathrm{s}}\boldsymbol{K}_s^{-1}\boldsymbol{K}_{sb}\dot{\boldsymbol{U}}_{\mathrm{b}}$. Considering that the coefficient α is generally <1, and velocity is smaller than acceleration in an earthquake, and taking into account the dynamic amplification effect, the response produced by $-(\boldsymbol{C}_{\mathrm{sb}} + \boldsymbol{C}_{\mathrm{s}}\boldsymbol{\Gamma}_{sb})\,\dot{\boldsymbol{U}}_{\mathrm{b}}$ will be less than that produced by $\boldsymbol{M}_{\mathrm{s}}\boldsymbol{\Gamma}_{sb}\ddot{\boldsymbol{U}}_b$, so the smaller one can be ignored for approximation purposes. Therefore, for an ordinary

structure without dampers, the acceleration model is more accurate than the displacement model in calculation and is not affected by elemental division, so it can be considered an exact method for seismic analysis of long-span structures.

Concentrated damping exists in structures when additional dampers or isolation devices are installed. Here, we assume that dampers are installed in the connections between the upper parts and supports, introducing matrix $\boldsymbol{C}_{\mathrm{d1}}$ and $\boldsymbol{C}_{\mathrm{d2}}$ to Eq. (1), in which $\boldsymbol{C}_{\mathrm{d1}}$ is an additional term of $\boldsymbol{C}_{\mathrm{sb}}$, and $\boldsymbol{C}_{\mathrm{d2}}$ is an additional term of $\boldsymbol{C}_{\mathrm{s}}$. If dampers exist within internal parts of the structure (not at the supports), we define the damping term $\boldsymbol{C}_{\mathrm{d3}}$, which corresponds to an additional term of $\boldsymbol{C}_{\mathrm{s}}$. Based on the above hypothesis, the ignored damping term in acceleration model can be expressed as

$$-\left(\boldsymbol{C}_{\mathrm{sb}}+\boldsymbol{C}_{\mathrm{s}}\boldsymbol{\Gamma}_{sb}\right)\dot{\boldsymbol{U}}_{\mathrm{b}}=\alpha\boldsymbol{M}_{\mathrm{s}}\boldsymbol{\Gamma}_{sb}\dot{\boldsymbol{U}}_{\mathrm{b}}-\boldsymbol{C}_{d1}\dot{\boldsymbol{U}}_{\mathrm{b}}-\left(\boldsymbol{C}_{\mathrm{d2}}+\boldsymbol{C}_{d3}\right)\boldsymbol{\Gamma}_{sb}\dot{\boldsymbol{U}}_{\mathrm{b}} \tag{20}$$

From the above analysis and Eq. (20), it can be observed that the error of the conventional acceleration model is mainly due to concentrated damping and has little relationship to mass damping. Therefore, the acceleration model may produce obvious errors in analysis of a structure with dampers installed. The error magnitude depends on many factors and is usually difficult to describe using Eq. (20), so a numerical analysis is presented later in this paper to examine it.

The damping approximation in the displacement and acceleration models produces some error and the magnitude of the error is different in different situations. The error magnitudes and distributions of the two models are also different from each other for the same structure. In summary, the error of the displacement model is associated with the damping term, corresponding to the structural parts connected with supports, despite too fine an elemental division. The ignored damping term cannot be eliminate in the calculation. The error of the acceleration model is associated with concentrated damping no matter where the damping concentrates and how the structural elements are divided. The errors and applicable ranges of the displacement model and the acceleration model can be summarized as follows: the displacement model is suitable for both linear and nonlinear analysis, too fine an elemental division of the structural bottom will produce some error, and the error is obviously influenced by the degree of elemental division. When dampers exist in the structure and damping concentrates in the parts connected to supports, it will also produce some error. However, because of the superposition principle adopted in the derivation of the acceleration model, it is only suitable for linear analysis and has good computational accuracy except when concentrated damping exists in structure.

4 Modification of calculation model

In view of the errors inherent in the displacement model and the acceleration model, both the time history and stochastic analysis methods should be modified to obtain accurate results and to facilitate error assessment for conventional calculation models. Corresponding software implementations are also briefly discussed in this section. The derivation of the stochastic analysis method makes use of the computationally efficient and accurate pseudo-excitation method.

4.1 Time history analysis

Accurate time history analysis by the displacement model should take into account the damping term $-\boldsymbol{C}_{\mathrm{sb}}\dot{\boldsymbol{U}}_{\mathrm{b}}$, which requires adopting Eq. (3) to carry out the calculation. In nonlinear

analysis, the stiffness term $-\boldsymbol{K}_{\mathrm{sb}}\boldsymbol{U}_{\mathrm{b}}$ and the damping term $-\boldsymbol{C}_{\mathrm{sb}}\dot{\boldsymbol{U}}_{\mathrm{b}}$ need to be considered simultaneously. In linear analysis, superposition of the following two equations can be used:

$$\boldsymbol{M}_{\mathrm{s}}\ddot{\boldsymbol{U}}_{s,1} + \boldsymbol{C}_{\mathrm{s}}\dot{\boldsymbol{U}}_{s,1} + \boldsymbol{K}_{\mathrm{s}}\boldsymbol{U}_{s,1} = -\boldsymbol{K}_{\mathrm{sb}}\boldsymbol{U}_{\mathrm{b}} \tag{21a}$$

$$\boldsymbol{M}_{\mathrm{s}}\ddot{\boldsymbol{U}}_{s,2} + \boldsymbol{C}_{\mathrm{s}}\dot{\boldsymbol{U}}_{s,2} + \boldsymbol{K}_{\mathrm{s}}\boldsymbol{U}_{s,2} = -\boldsymbol{C}_{\mathrm{sb}}\dot{\boldsymbol{U}}_{\mathrm{b}} \tag{21b}$$

in which $\boldsymbol{K}_{\mathrm{sb}}$ is the stiffness coefficient. $\boldsymbol{C}_{\mathrm{sb}}$ is the damping coefficient that incorporates not only Raleigh damping but also concentrated damping. According to Eq. (21), the accurate response is

$$\boldsymbol{U}_s = \boldsymbol{U}_{s,1} + \boldsymbol{U}_{s,2} \tag{22}$$

Using engineering software for seismic analysis and design of long-span structure, superposition is also available in linear situations, and accurate results consist of $\boldsymbol{U}_{s,1}$ produced by the displacement model and $\boldsymbol{U}_{s,2}$ produced by the concentrated damping force. It should be noted that while the range of ground acceleration between two discrete time points is assumed to be linear, the corresponding displacement curve must be a cubic spline function. To obtain more reasonable results when using ground displacement in seismic analysis, either a higher-order integration algorithm or a smaller integration time step is needed. The same is true when adopting ground velocity as the input in the calculation.

Similarly, accurate time history analysis by the acceleration model should take into account the damping term $-\left(\boldsymbol{C}_{\mathrm{sb}} + \boldsymbol{C}_{\mathrm{s}}\boldsymbol{\Gamma}_{sb}\right)\dot{\boldsymbol{U}}_{\mathrm{b}}$, that is:

$$\boldsymbol{M}_{\mathrm{s}}\ddot{\boldsymbol{U}}_s^d + \boldsymbol{C}_{\mathrm{s}}\dot{\boldsymbol{U}}_s^d + \boldsymbol{K}_{\mathrm{s}}\boldsymbol{U}_s^d = -\boldsymbol{M}_{\mathrm{s}}\boldsymbol{\Gamma}_{sb}\ddot{\boldsymbol{U}}_b - \left(\boldsymbol{C}_{\mathrm{sb}} + \boldsymbol{C}_{\mathrm{s}}\boldsymbol{\Gamma}_{sb}\right)\dot{\boldsymbol{U}}_{\mathrm{b}} \tag{23}$$

in which $\boldsymbol{C}_{\mathrm{sb}}$ and $\boldsymbol{C}_{\mathrm{s}}$ are damping coefficients that incorporate both Raleigh damping and concentrated damping, meaning that dampers exist in structure. The conventional acceleration model in Eq. (8) can provide sufficiently accurate results when only Raleigh damping exists. However, concentrated damping may lead to some error. Thus, structural seismic response with complex damping consisting of two parts is considered as follows:

$$\boldsymbol{M}_{\mathrm{s}}\ddot{\boldsymbol{U}}_{s,1}^d + \boldsymbol{C}_{\mathrm{s}}\dot{\boldsymbol{U}}_{s,1}^d + \boldsymbol{K}_{\mathrm{s}}\boldsymbol{U}_{s,1}^d = -\boldsymbol{M}_{\mathrm{s}}\boldsymbol{\Gamma}_{sb}\ddot{\boldsymbol{U}}_b \tag{24a}$$

$$\boldsymbol{M}_{\mathrm{s}}\ddot{\boldsymbol{U}}_{s,2}^d + \boldsymbol{C}_{\mathrm{s}}\dot{\boldsymbol{U}}_{s,2}^d + \boldsymbol{K}_{\mathrm{s}}\boldsymbol{U}_{s,2}^d = -\left(\boldsymbol{C}_{\mathrm{sb}} + \boldsymbol{C}_{\mathrm{s}}\boldsymbol{\Gamma}_{sb}\right)\dot{\boldsymbol{U}}_{\mathrm{b}} \tag{24b}$$

An accurate response consists of the results in Eq. (24):

$$\boldsymbol{U}_s = \boldsymbol{U}_{s,1}^d + \boldsymbol{U}_{s,2}^d + \boldsymbol{\Gamma}_{sb}\boldsymbol{U}_b \tag{25}$$

Thus, using engineering software to calculate the seismic response of a long-span structure requires linear superposition, which is the combination of $\boldsymbol{U}_{s,1}^d + \boldsymbol{\Gamma}_{sb}\boldsymbol{U}_b$ produced by the conventional acceleration model and $\boldsymbol{U}_{s,2}^d$ produced by the additional concentrated damping force.

4.2 Stochastic analysis

The pseudo-excitation method, proposed and developed by Lin (1992), is an efficient and accurate method for stochastic analysis of structures and has been widely applied in scientific research and engineering practice. Therefore, instead of the traditional stochastic method, the pseudo-excitation method is adopted in this study to calculate structural response to multi-point earthquake excitation. First, the power spectral density function matrix of ground

displacement in an earthquake is defined as $\boldsymbol{S}_{\boldsymbol{U}_b}$, with order $l \times l$ and l supports. $\boldsymbol{S}_{\boldsymbol{U}_b}$ must be the Hermitian matrix, so it can be decomposed into

$$\boldsymbol{S}_{\boldsymbol{U}_b} = \sum_{j=1}^{l} \lambda_j \boldsymbol{\psi}_j \boldsymbol{\psi}_j^{*T} \tag{26}$$

in which superscripts $*$ and T respectively represent conjugation and transposition of the matrix. λ_j and $\boldsymbol{\psi}_j$ represent the eigenvalue and eigenvector of $\boldsymbol{S}_{\boldsymbol{U}_b}$. l is the number of supports. Thus, pseudo-excitation can be constructed using the following eigenpair:

$$\tilde{\boldsymbol{U}}_{bj} = \boldsymbol{\psi}_j^* \sqrt{\lambda_j} e^{r\omega t}, \quad r = \sqrt{-1} \tag{27}$$

In the modified displacement model, the pseudo response is given by Eq. (21):

$$\tilde{\boldsymbol{U}}_{sj} = \boldsymbol{H}\left(\boldsymbol{K}_{sb} + \boldsymbol{C}_{sb} r\omega\right) \tilde{\boldsymbol{U}}_{bj} \tag{28}$$

in which $\boldsymbol{H} = -\left(\boldsymbol{K}_s - \omega^2 \boldsymbol{M}_s + r\omega \boldsymbol{C}_s\right)^{-1}$. In the conventional displacement model, the corresponding pseudo response is $\tilde{\boldsymbol{U}}_{sj} = \boldsymbol{H}\boldsymbol{K}_{sb}\tilde{\boldsymbol{U}}_{bj}$. Thus, the power spectral density function matrix of structural response $\boldsymbol{U}_s$ can be expressed as

$$\boldsymbol{S}_{\boldsymbol{U}_s} = \sum_{j=1}^{l} \tilde{\boldsymbol{U}}_{sj}^* \tilde{\boldsymbol{U}}_{sj}^T \tag{29}$$

The mean square value and root mean square value of the structural response $\boldsymbol{U}_s$ can be obtained by integration of the power spectral density function in Eq. (29).

In the modified acceleration model, the pseudodynamic response is given by combining Eqs. (24) and (25):

$$\tilde{\boldsymbol{U}}_{sj}^d = \boldsymbol{H}\left[\boldsymbol{M}_s \boldsymbol{\Gamma}_{sb} \omega^2 + \left(\boldsymbol{C}_{sb} + \boldsymbol{C}_s \boldsymbol{\Gamma}_{sb}\right) r\omega\right] \tilde{\boldsymbol{U}}_{bj} \tag{30}$$

in which all parameters have been defined previously. Unlike in Eq. (30), the corresponding pseudodynamic response in the conventional acceleration model is $\tilde{\boldsymbol{U}}_{sj}^d = \boldsymbol{H}\boldsymbol{M}_s \boldsymbol{\Gamma}_{sb} \omega^2 \tilde{\boldsymbol{U}}_{bj}$. Taking into account both the pseudostatic response and pseudodynamic response, the total pseudo response is given by

$$\tilde{\boldsymbol{U}}_{sj} = \tilde{\boldsymbol{U}}_{sj}^d + \boldsymbol{\Gamma}_{sb} \tilde{\boldsymbol{U}}_{bj} \tag{31}$$

In the modified acceleration model, the pseudo response is calculated using Eqs. (30) and (31), and the power spectral density function is calculated using Eq. (29). The mean square value and root mean square value of the structural response can be obtained by integration of the power spectral density function. In this discussion of the model modification using the pseudo-excitation method for high efficiency, it should be noted that using engineering software is difficult to employ the pseudo excitation method and achieve further stochastic modification.

5 Numerical study

A simple example of a long-span structure is established to conduct a numerical study of error situations with the displacement model and the acceleration model. Vigorous theoretical derivations can be verified by numerical calculations and error situations, magnitudes, distributions and key influencing parameters can all be analyzed by numerical analysis. A long-span

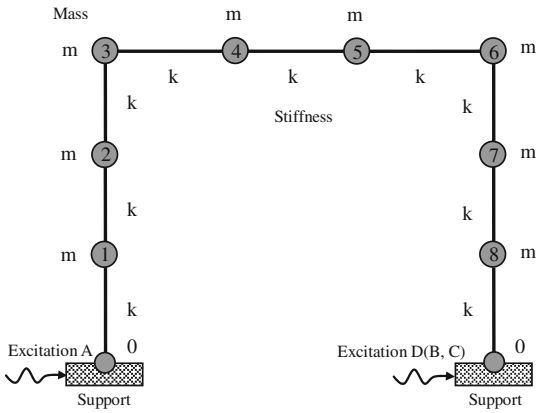

Fig. 2 Schematic diagram of long-span structure model

Table 1 Parameters of long-span structure and dampers

Parameter of long-span structure	Mass m/kg	2.0×10^5
	Stiffness k /N m^{-1}	1.0×10^6
	Damping ratio of the first two modes	0.05
Parameter of dampers	Damping coefficient c_d/N s m^{-1}	1.0×10^6
Position of dampers	Configuration 1	[0, 1], [0, 8]
	Configuration 2	[1, 3], [6, 8]
	Configuration 3	[1, 5], [4, 8]
	Configuration 4	[2, 4], [5, 7]
	Configuration 5	[2, 6], [3, 7]

structure with uniform distributions of mass and stiffness is assumed for this example and is described by a numerical model with multiple nodes. The nodes are numbered from 1 to 8, as shown in Fig. 2. Assumptions of lumped mass and Rayleigh damping are adopted. Corresponding structural parameters are listed in Table 1. By installing dampers in the structure to achieve concentrated damping, the accuracy of the structural responses calculated by the displacement model and by the acceleration model is studied. There are five damper layout configurations expressed by structural node marks connecting two damper ends, such as [a, b], which means that the damper connects with structural node a and node b, in which a and b are both node marks. All damper layout configurations are also listed in Table 1. It can be observed that additional dampers connect with not only adjacent nodes but also non-adjacent nodes to study the influence of different damper layout configurations on the accuracy of the calculation models. From the derivations presented in previous sections of this paper, it can be observed that the stiffness of the dampers does not affect the accuracy of the calculation models; for this numerical example, the stiffness of the dampers is set to zero and only damping coefficients are considered. Corresponding parameter values of the dampers are shown in Table 1. Because of the lack of suitable actual earthquake records, it is usually difficult to find a suitable multi-point ground motion to excite structure. Thus, we develop a simulation procedure to generate artificial multi-point ground motion in an earthquake, and referring to China's seismic code, the relevant parameter settings are the following: the earthquake is a rare 8 degrees; the site class is II; the modified Clough–Penzien power spectral model is

adopted, as is the Hao coherent model (which yields good simulation effects in the range of one hundred meters); and the seismic apparent wave velocity is 400 m/s. To analyze the seismic responses of structures with different spans, a program was developed to generate a four-point equally spaced earthquake excitation, with the four points as point A (0 m), point B (100 m), point C (200 m), point D (300 m). The acceleration, velocity and displacement time histories of the four points are shown in Fig. 3. Baseline adjustment of the displacement time history is also conducted. Figures 4, 5, 6 illustrate the degree of fit of the power spectral density functions, the coherent coefficients and the response spectra of the simulated multi-point earthquake excitation. These figures show that the generated multi-point earthquake excitation is suitable and appropriate. The four-point ground motion was used to construct several combinations of earthquake excitations, expressed as [A, A], [A, B], [A, C] and [A, D], in which, for example, [A, D] refers to adopting points A and D as the multi-point input. To facilitate the presentation below, four calculation models adopted for seismic analysis of long-span structures are expressed as follows: the displacement model is abbreviated as DM, the acceleration model is abbreviated as AM, the modified displacement model is abbreviated as M-DM, and the modified acceleration model is abbreviated as M-AM. According to the theoretical derivations presented in previous sections, the results obtained from M-DM and M-AM can be considered accurate values and thus can be used to assess the accuracy of DM and AM.

5.1 Ordinary structure with Rayleigh damping characteristic

The accuracy of the displacement model and the acceleration model in calculation of the seismic response of an ordinary structure with Rayleigh damping is examined in this section. Earthquake combination [A, D] is adopted as the multi-point input, and the structural parameter settings in Table 1 are used assuming no dampers are installed in structure. In seismic analysis and structural design, internal forces between adjacent nodes are closely related to relative displacements, so here, relative displacement is used as an index, and four representative nodes numbered 1, 8, 4, 5 are selected for consideration in the analysis. Figure 7 shows the relative displacements of nodes 1, 8, 4, 5 as calculated by DM, AM, M-DM and M-AM, respectively. For nodes 1 and 8, the displacement relative to corresponding connected supports is adopted; for node 4, the displacement relative to node 3 is adopted; and for node 5, the displacement relative to node 6 is adopted. Figure 7 illustrates clearly that the time history responses given by the four calculation models are nearly coincident. This implies that both displacement model and the acceleration model are sufficiently accurate and that the calculated results do not need to be corrected. This is why the displacement model and the acceleration model are often used in design and analysis by most researchers and engineers: both of the models are accurate enough to calculate the seismic response of ordinary structures.

The structural parameter settings in Table 1 are taken as case 1. We can divide the long span structure into models composed of several elements. The following five additional cases are defined in terms of the number of elements into which the structure is divided: case 2, number of nodes $n = 16$, node mass $m_s = 2 \times 10^5/(16/8)$kg, element stiffness $k_s = 1 \times 10^6 \times (16/8)$ N/m; case 3, number of nodes $n = 32$, node mass $m_s = 2 \times 10^5/(32/8)$kg, element stiffness $k_s = 1 \times 10^6 \times (32/8)$ N/m; case 4, number of nodes $n = 64$, node mass $m_s = 2 \times 10^5/(64/8)$kg, element stiffness $k_s = 1 \times 10^6 \times (64/8)$ N/m; case 5, number of nodes $n = 128$, node mass $m_s = 2 \times 10^5/(128/8)$kg, element stiffness $k_s = 1 \times 10^6 \times (128/8)$ N/m; and case 6, number of nodes $n = 256$, node mass $m_s = 2 \times 10^5/(256/8)$kg, element stiffness $k_s = 1 \times 10^6 \times (256/8)$ N/m. Node 1 is taken as an example, and DM,

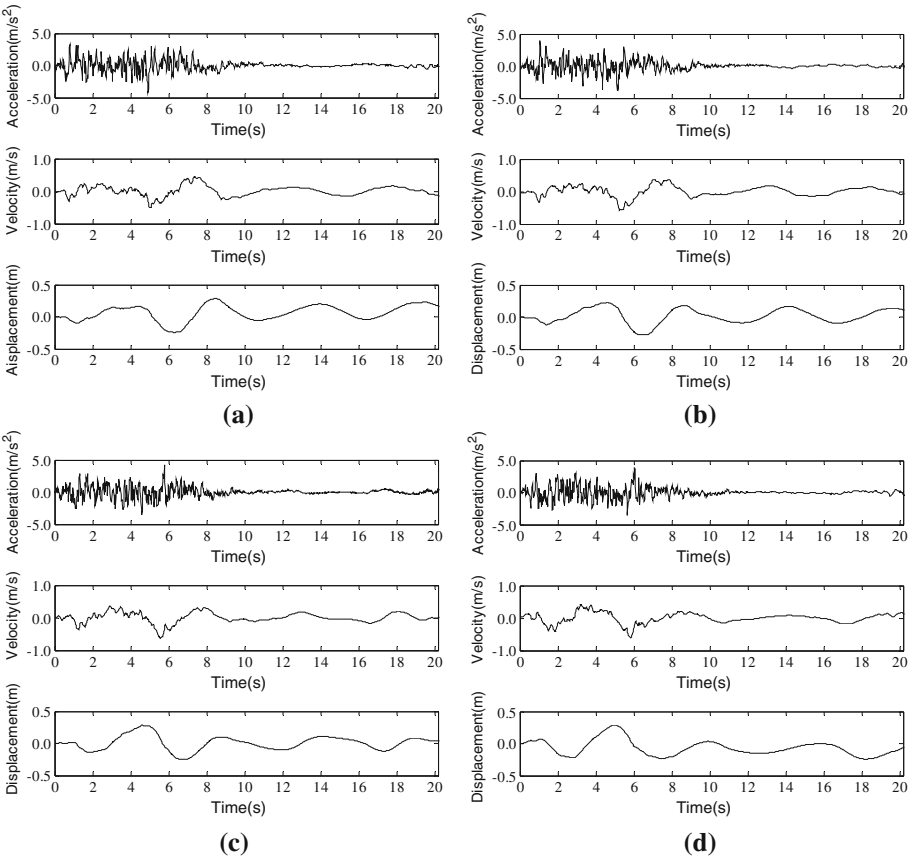

Fig. 3 Acceleration, velocity, displacement time histories of simulated multi-point ground motion. **a** Point A, **b** point B, **c** point C, **d** point D

AM, M-DM and M-AM are applied as calculation models. The displacement time histories of node 1 relative to its support (shown as node 0 in Fig. 2) are calculated for cases 1 to 6. To obtain accurate results, a high-order iterative algorithm should be used with the displacement time history as the external input. This is because ground displacement actually follows a cubic spline function corresponding to the linear variation of ground acceleration between neighboring time points. Figure 8 shows the curves of the calculation results corresponding to the six cases. Some errors exist where bottom elements of the structure are too finely divided, and the more finely divided the elements are, the larger the calculation errors of the displacement model are. These results agree well with the theoretical derivations presented in Sect. 3.1. In Fig. 8, the error produced by the displacement model approaches or exceeds 100 % when the numbers of nodes n = 128, 256. This means that there will be a large error in the corresponding bottom shear, which may lead to overly conservative seismic design. We next adopt as an example, case 5 with 128 nodes, for which the displacement model produces significant apparent errors. In similar fashion to that shown in Fig. 2, the structural nodes for case 5 are numbered counterclockwise from 1 to 128. We select a series of nodes (1, 2, 8, 16, 32, 64, 127, and 128) and adopt a series of corresponding neighboring nodes (0, 3, 9, 17, 33, 65, 126, and 0). We use a variety of seismic combinations ([A, A], [A, B], [A, C] and [A, D]) as

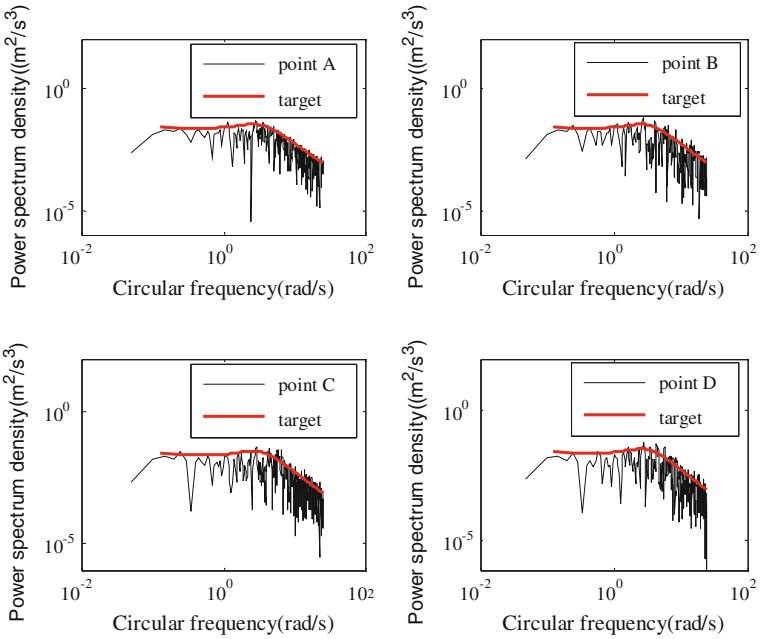

Fig. 4 Comparison of simulated and target power spectrum density of multi-point ground motion

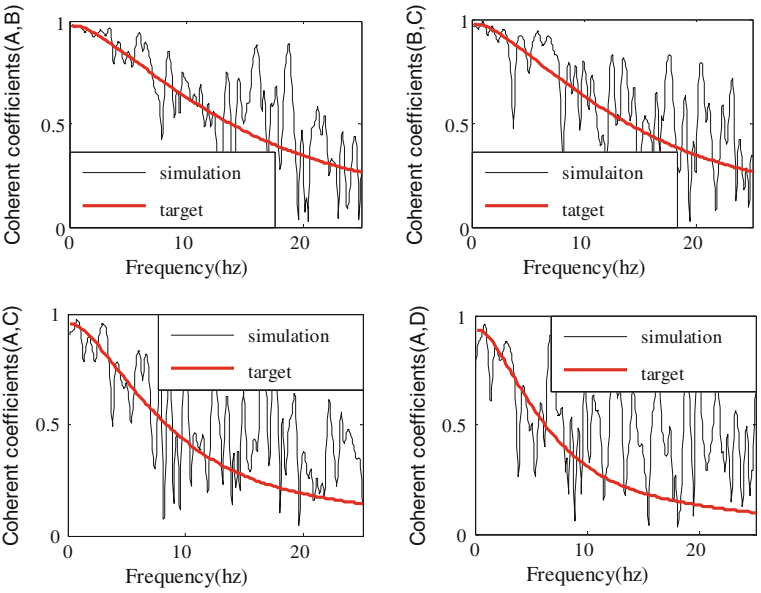

Fig. 5 Comparison of simulated and target coherence coefficients of multi-point ground motion

multi-point inputs, and we calculate the maximum values of the relative displacements of the selected nodes using the four models (DM, AM, M-DM and M-AM). The results are shown in Fig. 9. Obvious error exists in the relative displacements of the structural bottom elements for

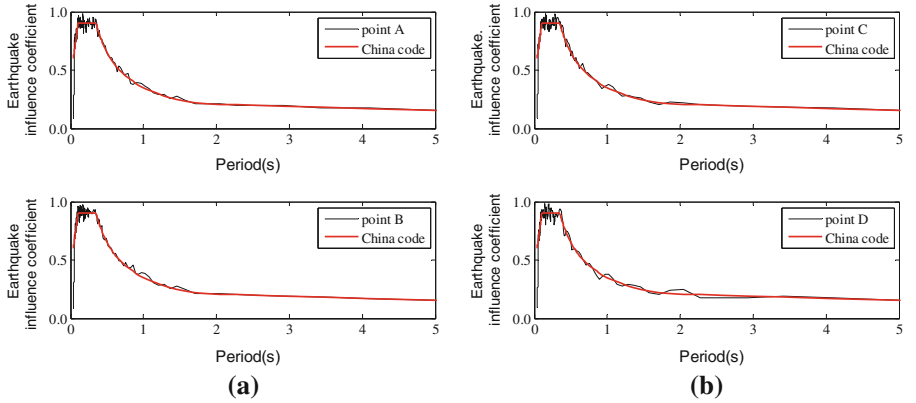

Fig. 6 Comparison of simulated and design response spectrum of multi-point ground motion in seismic code of China. **a** Earthquake response spectrum at point A and B, **b** earthquake response spectrum at point C and D

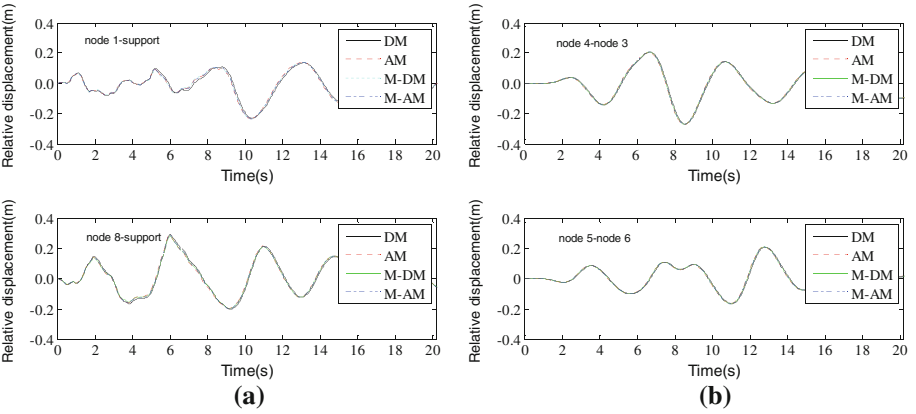

Fig. 7 Displacement time histories of node 1, 8, 4 and 5 in ordinary structure with Rayleigh damping based on four seismic calculation models. **a** Node 1 and 8. **b** Node 4 and 5

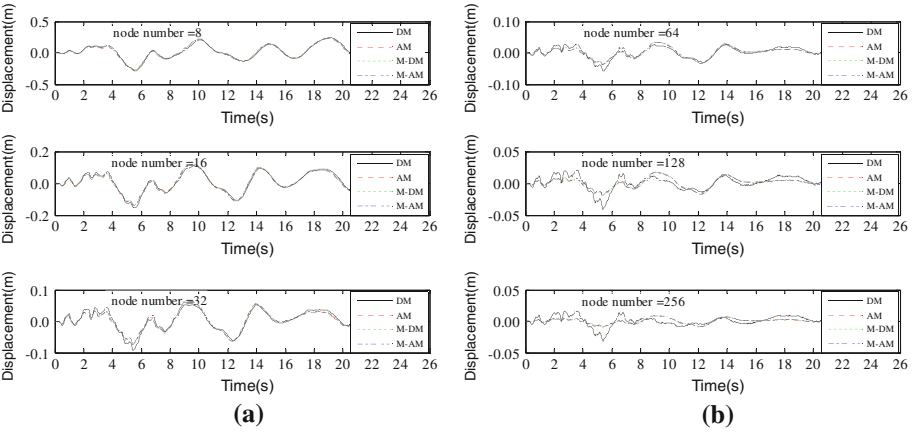

Fig. 8 Displacement time histories of node 1 of ordinary structure under different element divisions. **a** Node number 8, 16 and 32. **b** Node number 64,128 and 256

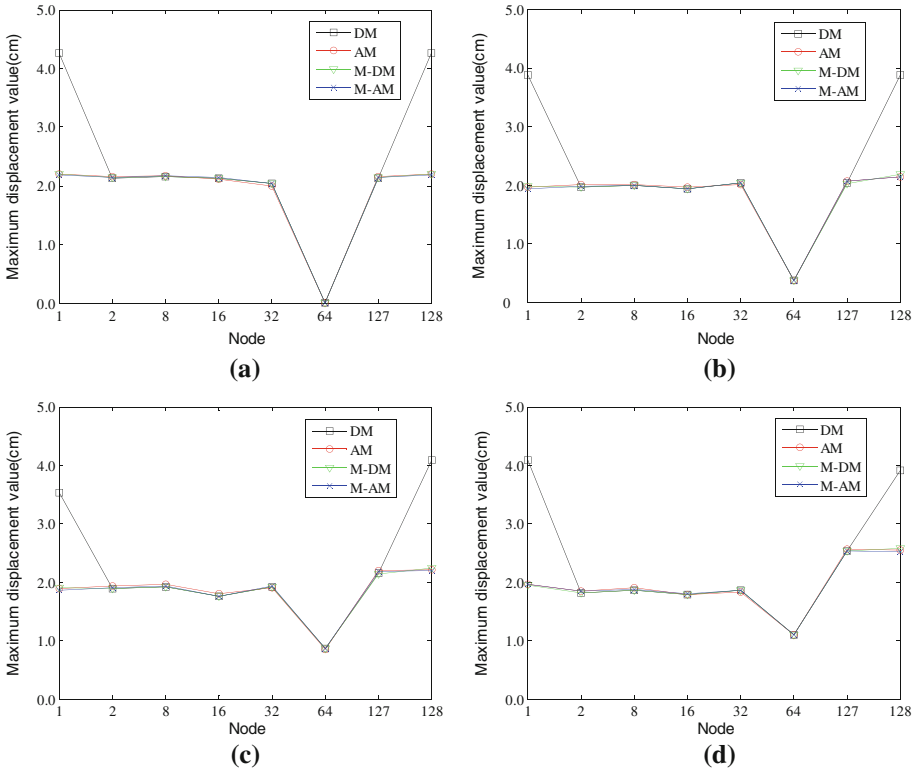

Fig. 9 Maximum displacement responses of several structural nodes subjected to different seismic combinations based on four seismic calculation models. **a** Seismic combination [A, A], **b** seismic combination [A, B], **c** seismic combination [A, C], **d** seismic combination [A, D]

the displacement model when the structural bottom is too finely divided. Moreover, different earthquake excitations have different influences on the error situation, mainly in relation to the ratio between peak velocity and peak acceleration of ground motion (PGV/PGA). From Eq. (16) we know that the larger the PGV/PGA ratio, the larger the calculation error of the displacement model, so the error in the results calculated with the displacement model will be more apparent for cases in which the structural bottom is too finely divided and near-field ground motion consisting of a large velocity pulse is assumed. Figure 9 also shows that when bottom elements are too finely divided obvious error will exist in the internal force on the bottom elements calculated by the displacement model, even if uniform ground motion is assumed. Moreover, the calculation error tends to diverge increasingly from the correct solution as the bottom elements are more finely divided. Figure 9 also shows that the acceleration model always has good accuracy in seismic response calculation no matter how the structural elements are divided. This can be explained by the theoretical derivations presented in previous sections: for an ordinary structure with Rayleigh damping, the influence of the ignored damping term on the accuracy of the acceleration model is small, and mass damping is also relative small, so the calculation error can be neglected. In general, some error exists in the displacement model's seismic response calculation for ordinary structures with Rayleigh damping, and this error becomes more obvious as the bottom elements are more finely divided. In contrast to the responses obtained from the displacement model,

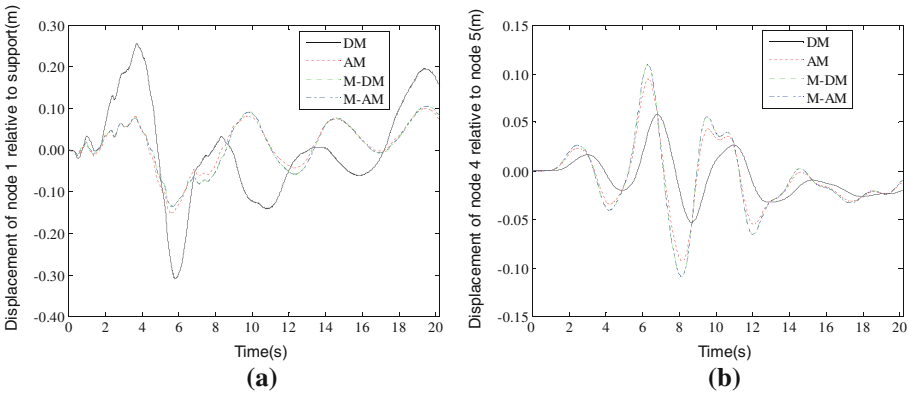

Fig. 10 Displacement time histories of node 1 and 4 based on four seismic calculation models while the concentrated damping characteristic exists at the bottom of structure. **a** Node 1. **b** Node 4

the seismic responses of ordinary structures obtained from the acceleration model can be considered accurate.

5.2 Structure with concentrated damping existing at the bottom

When dampers are installed at the bottom of a structure, concentrated damping exists near the supports. Case 1 (8 nodes) is selected as an example of a structure that can avoid error produced by too fine an elemental division. The structural parameters and damper configuration corresponding to case 1 are listed in Table 1. The excitation for this example is seismic combination [A, D]. Figure 10 shows the relative displacement time histories of nodes 1 and 4 obtained from four calculation models. Node 1 represents a bottom node, and its displacement is relative to its support (node 0). Node 4 represents an internal node, and its displacement is relative to node 5. Figure 10 shows that when concentrated damping exists at the bottom of the structure, the displacement model will yield erroneous results even if the bottom elements are not too finely divided. In this numerical example, the degree of error exceeds 100 %, and the errors produced by the displacement model exist not only in the bottom nodes but also in the internal nodes of the structure, as is the case for node 4 as shown in Fig. 10b. This figure also shows that the acceleration model is relatively more accurate than the displacement model. It should be remembered that regardless of whether the displacement model or the acceleration model is adopted, concentrated damping at supports can also cause calculation error independent of the degree of elemental division. Here, concentrated damping at supports means that there are dampers connecting bottom elements or internal elements with supports.

To further study error situations for the calculation models, a variety of seismic combinations ([A, A], [A, B], [A, C] and [A, D]) are adopted, and the maximum values of the seismic response of all structural nodes are considered. Nodes 0, 3, 4, 5, 6, 7, 8, and 0 are selected as neighbors for nodes 1, 2, 3, 4, 5, 6, 7, 8, respectively, where 0 denotes a support. The calculation results are shown in Fig. 11. For all of the seismic combinations studied, relative displacements of the structural nodes, as calculated by the displacement model, have obvious error. Different seismic combinations have different calculation errors. The calculation error of the displacement model exists not only for the bottom elements but also for the internal elements of structure. The calculated seismic response at the bottom is greater than the correct value, and the calculated response at internal elements of the structure is smaller than the

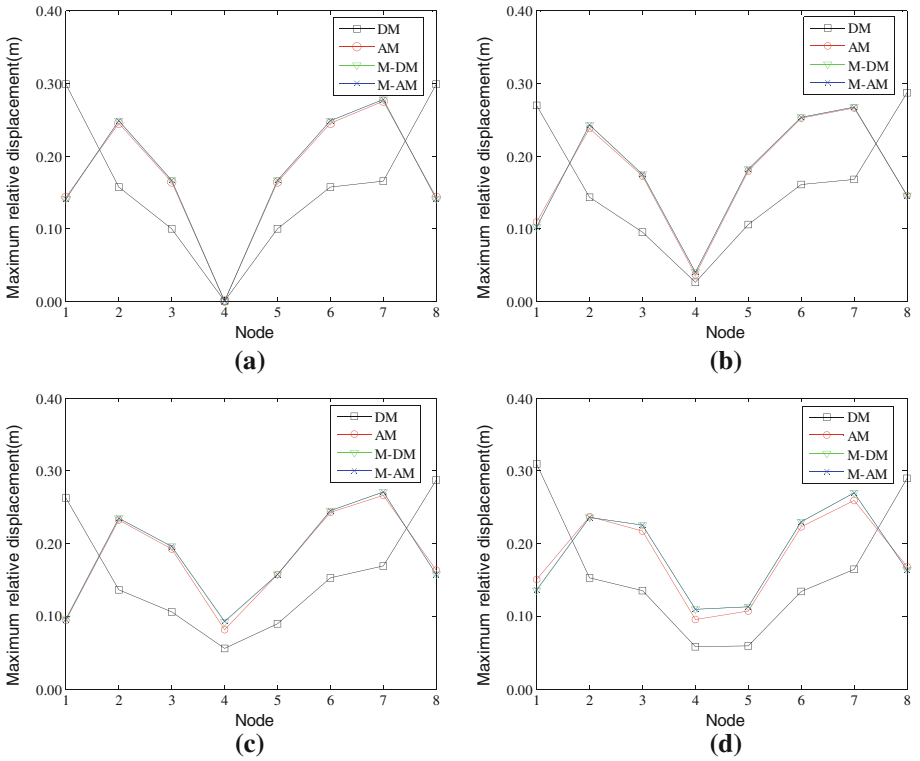

Fig. 11 Maximum displacement responses of all structural nodes subjected to different seismic combinations based on four seismic calculation models while the concentrated damping characteristic exists at the bottom of structure. **a** Seismic combination [A, A], **b** Seismic combination [A, B], **c** Seismic combination [A, C], **d** Seismic combination [A, D]

value. The seismic response calculated by the acceleration model is also inaccurate, but the error is small compared with that produced by the displacement model. Figure 11 shows that even when seismic combination [A, A], denoting uniform input, is adopted, some error still exists with the acceleration model. This is mainly because the static transformation matrix $\boldsymbol{\Gamma}_{sb} = -\boldsymbol{K}_s^{-1}\boldsymbol{K}_{sb}$ is adopted in the calculation. If $\boldsymbol{\Gamma}_{sb} = I$ and mass damping is neglected, it does not produce any error. In this situation, the acceleration model actually equals Eq. (9), which is usually used in seismic analysis.

Setting dampers at the bottom of structure, error situations corresponding to different damping coefficients can be studied. We define a constant value $\mathrm{CD} = 1 \times 10^6\ \mathrm{N} \times \mathrm{m} \times \mathrm{s}^{-1}$, and accordingly, we adopt four damping coefficients: $\mathrm{c_d} = [1, 5, 10, 20] \times \mathrm{CD}$, and seismic combination [A, D]. We select two representative nodes, 1 and 4, and the displacements of the two nodes relative to nodes 0 and 5, respectively, are selected as indices. Figure 12 shows the change in the maximum values of the seismic displacement responses of nodes 1 and 4 with increasing damping coefficient. It can be observed that the larger the damping coefficient, the more apparent the calculation error of the displacement model. When the acceleration model is adopted in the seismic calculation and $\mathrm{c_d} = 20 \times 10^6\ \mathrm{N} \times \mathrm{m} \times \mathrm{s}^{-1}$, the errors corresponding to nodes 1 and 4 are also obvious. Therefore, we conclude that increasing the damping coefficients provided by dampers leads to increasing error with the displacement model, which is consistent with the findings from the theoretical derivations and

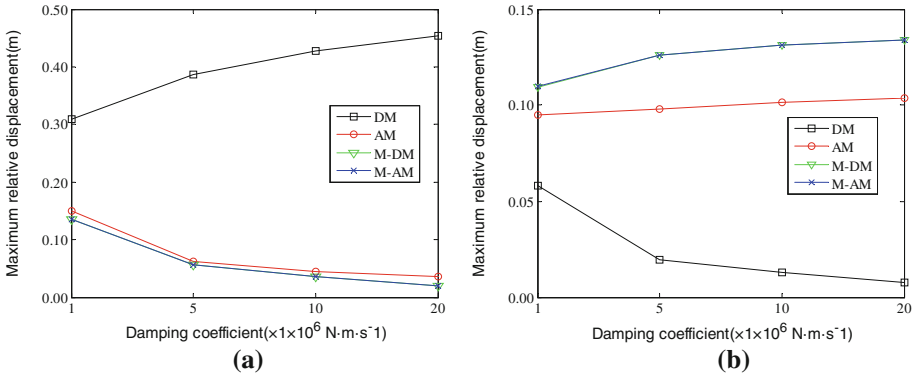

Fig. 12 Maximum displacement responses of node 1 and 4 corresponding to different damping coefficients at the bottom of structure based on four seismic calculation models. **a** Node 1. **b** Node 4

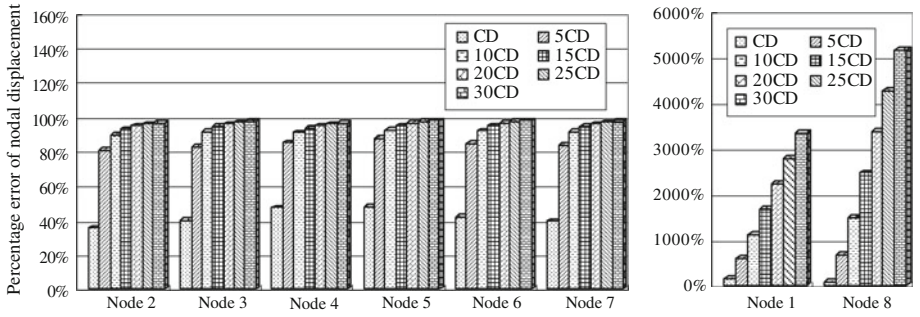

Fig. 13 Error of calculation responses of all structural nodes corresponding to different damping coefficients at the bottom of structure based on displacement model

numerical analyses presented in previous sections. However, increasing damping coefficients has little influence on the accuracy of the acceleration model, although the errors still increase accordingly. To further study error situations of the displacement model and the acceleration model, we define error indices ρ_{DM} and ρ_{AM}:

$$\rho_{DM} = \text{abs}\left(\max|u_{DM}| - \max|u_{M\text{-}DM}|\right)/\max|u_{M\text{-}DM}| \tag{32a}$$

$$\rho_{AM} = \text{abs}\left(\max|u_{AM}| - \max|u_{M\text{-}AM}|\right)/\max|u_{M\text{-}AM}| \tag{32b}$$

in which u_{DM} is the result calculated with the displacement model, u_{AM} is the result calculated with the acceleration model, $u_{M\text{-}DM}$ is the corrected result calculated with the modified displacement model, and $u_{M\text{-}AM}$ is the corrected result calculated with the modified acceleration model. Both $u_{M\text{-}DM}$ and $u_{M\text{-}AM}$ can be considered accurate results. The error index proposed in Eq. (32) does not consider positive and negative value changes because it only addresses the magnitude of error. Therefore, we assign seven damping coefficients, $c_d = [1, 5, 10, 15, 20, 25, 30] \times CD$, to the dampers. The relative displacements of all of the structural nodes are calculated, and the errors are further identified. The calculation model adopted is the same as in the previous sections. Figure 13 illustrates the error situations of the relative displacement time histories of the structure corresponding to the various damping coefficients considered. Obvious errors exist in the seismic responses of all structural nodes calculated by the displacement model. For bottom elements of the structure, as the

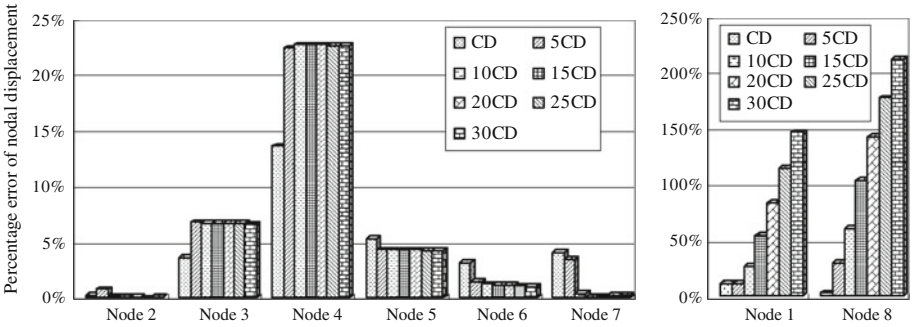

Fig. 14 Error of calculation responses of all structural nodes corresponding to different damping coefficients at the bottom of structure based on acceleration model

damping coefficient increases, the calculated displacement diverges increasingly from the correct value. For internal elements of the structure, the calculation error increases with the damping coefficient and approaches a stable value, and the errors for all of the internal nodes of the structure are similar. Figure 14 illustrates error situations for relative displacement time histories of the structure corresponding to several different damping coefficients, with the acceleration model adopted for the calculations. It can be observed that the acceleration model is more accurate than the displacement model. Increases in the damping coefficient correspond to increasingly obvious errors calculated with the acceleration model, most obviously for the bottom elements of the structure. In the numerical example, the maximum error at the bottom approaches 200 %. The errors for the internal elements of the structure are relatively small, and the maximum error for the internal elements is <25 %. The magnitude of error varies by element, but the errors for the internal nodes of the structure do not increase as the damping coefficient increases. This is mainly due to mutual cancellation of the ignored damping term in the acceleration model for internal nodes. In general, errors produced by the displacement model are obvious when dampers are installed at the supports, and increases in the damping coefficient correspond to increasing errors for bottom elements, while those of internal elements are relatively small and stable. When the acceleration model is applied to a structure equipped with dampers, increases in the damping coefficient correspond to some increase in errors for bottom elements, and errors for internal elements are small and unstable, although errors for some internal nodes may decrease. Thus, when concentrated damping exists at supports, both of the displacement model and the acceleration model need to be modified, especially for elements connected to supports.

5.3 Structure with concentrated damping existing in the internal parts of structure

When dampers are installed within the upper parts of a long-span structure, concentrated damping characteristics exist in internal parts of the structure. Damper configurations numbered 2–5 are listed in Table 1. From the theoretical derivations presented in previous sections, we know that when dampers are installed in internal parts of a structure its error mechanism is different from that when dampers are installed at the supports. Assuming that concentrated damping only exists in upper parts of the structure, a further numerical study on the range of applicability and error situations of the four calculation models (DM, AM, M-DM and M-AM) is conducted. The structure is assumed to be an 8-node model, and its parameters are listed in Table 1. The seismic excitation combination adopted is [A, D]. Damper

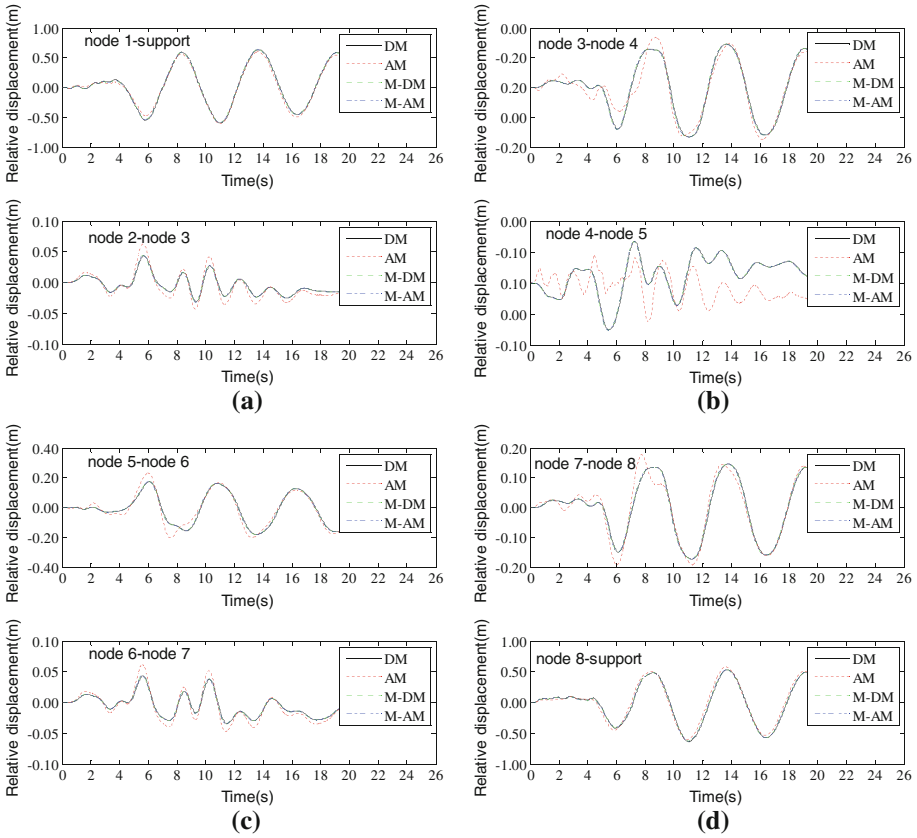

Fig. 15 Displacement time histories of all structural nodes based on four seismic calculation models while the concentrated damping characteristic exists within internal parts of structure. **a** Node 1 and 2. **b** Node 3 and 4. **c** Node 5 and 6. **d** Node 7 and 8

configuration 3 is used with a damping coefficient of $c_d = 10 \times 10^6$ N × m × s^{-1}. Nodes 1–8 are selected, and the indices are defined in terms of the relative displacements of these nodes. The corresponding neighboring nodes are 0, 3, 4, 5, 6, 7, 8, and 0, respectively. Figure 15 shows the relative displacement responses of the structural nodes. It can be observed that the acceleration model produces obvious errors except for nodes 1 and 8. However, in this case, the displacement model can be considered a nearly accurate calculation model, which can be explained by the theoretical derivation presented previously: when there is concentrated damping in internal parts of the structure, the ignored damping term $-\boldsymbol{C}_{sb}\dot{\boldsymbol{U}}_b$ in the displacement model only includes stiffness damping, which is small enough to be neglected. Therefore, the following analysis focuses primarily on the calculation error associated with the acceleration model.

Several damper configurations are used to study the error of the acceleration model. The parameter settings are similar to those above, and the damper configurations 2–5 adopted are summarized in Table 1. Maximum values of the relative displacement responses of the structural nodes are selected as indices to assess the accuracy of the acceleration model. Figure 16 shows the maximum values of the relative displacement responses of structural nodes based on the four calculation models and the different damper configurations. It can

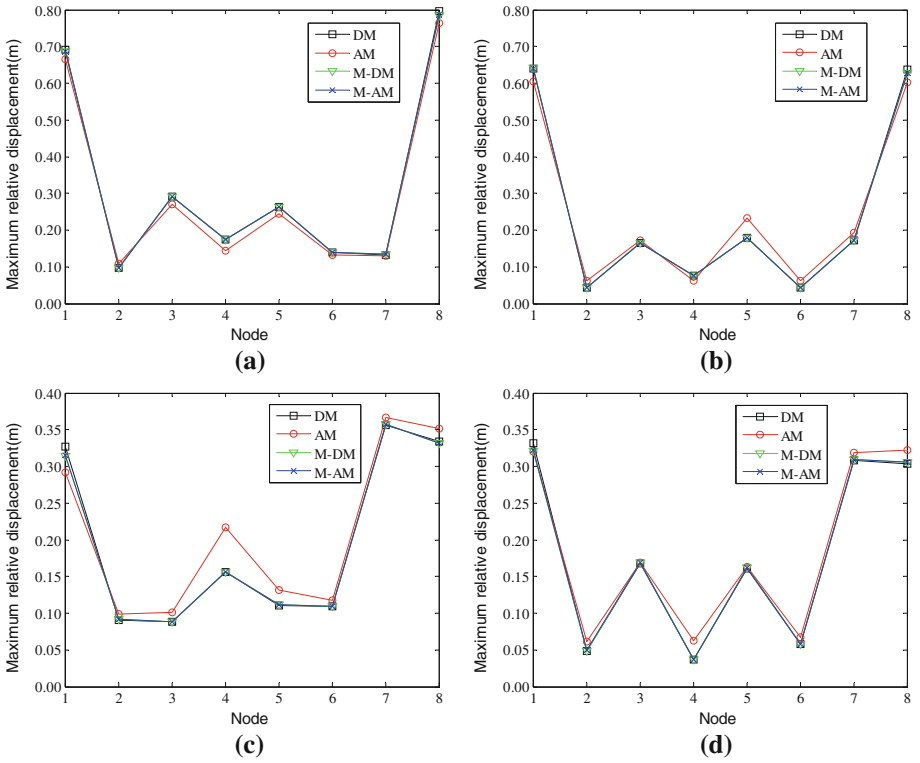

Fig. 16 Maximum displacement responses of all structural nodes corresponding to different damper configurations based on four seismic calculation models. **a** Configuration 2, **b** Configuration 3, **c** Configuration 4, **d** Configuration 5

be observed from Fig. 16 that there is some error produced by the acceleration model for all damper configurations, and the error is relatively obvious for internal parts of the structure. To clearly describe error situations of the acceleration model for different damper configurations, error indices ρ_{DM} and ρ_{AM} in Eq. (32) are adopted. Figure 17 describes the error situation for the acceleration model. It can be observed that errors in the displacement response of the same structural node vary greatly for different damper configurations. For example, errors for node 6 under different damper configurations are generally small, but the error corresponding to damper configuration 2 is 40 %. Moreover, errors for different nodes differ greatly for the same damper configuration. From the figure, it can also be observed that the errors produced by the acceleration model for bottom elements are relatively small, but the errors for internal elements of the structure are large. However, the relationship between error and damper configuration is difficult to describe and assess, and the errors produced by the acceleration model differ significantly for different damper configurations, so the acceleration model needs to be amended in practical engineering applications.

A variety of seismic combinations ([A, A], [A, B], [A, C] and [A, D]) and damper configuration 3, corresponding damping coefficient is $c_d = 10 \times 10^6\ N \times m \times s^{-1}$, are adopted for the next numerical analysis. The accuracy of the acceleration model is studied for different seismic combinations. Maximum values of the relative displacement responses of all structural nodes are adopted as indices, and 0, 3, 4, 5, 6, 7, 8, and 0 are selected as neighboring nodes for nodes 1, 2, 3, 4, 5, 6, 7, and 8, respectively, where 0 denotes support. Figure 18 shows the

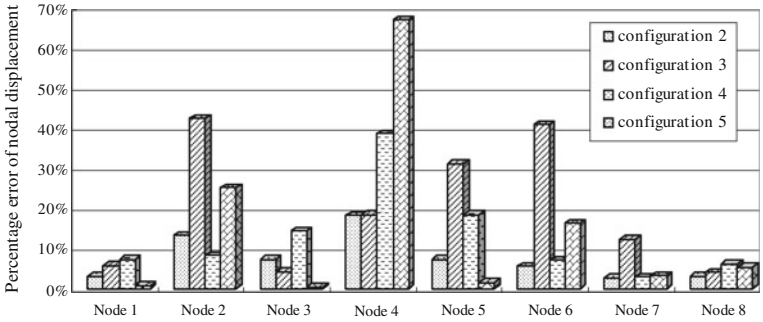

Fig. 17 Error of calculation responses of all structural nodes corresponding to different damping coefficients while concentrated damping exists in internal parts of structure based on acceleration model

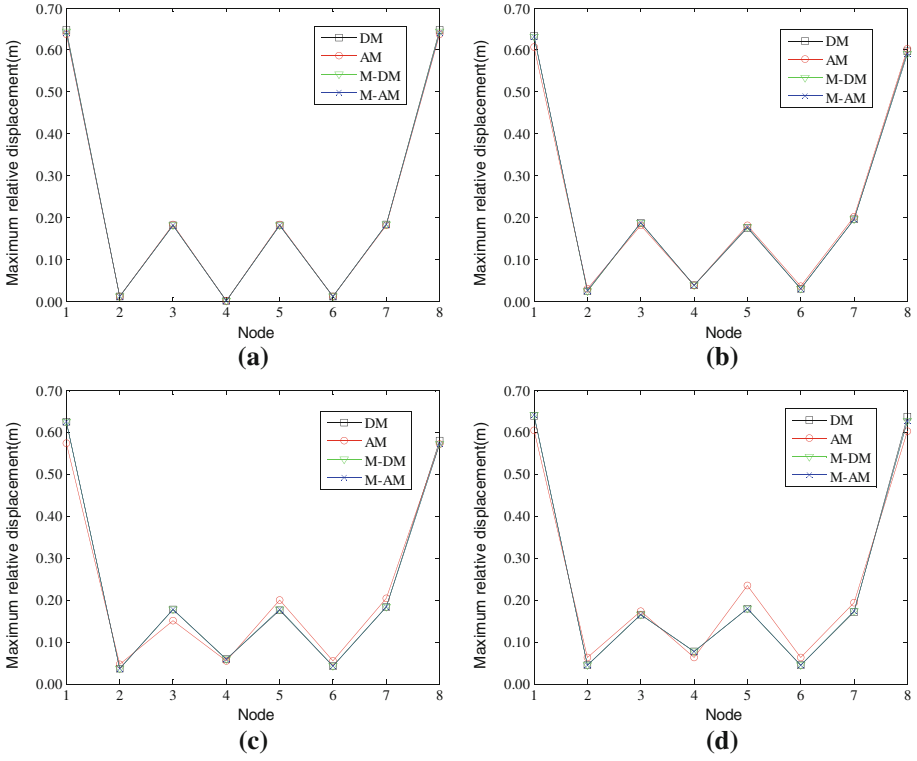

Fig. 18 Maximum displacement responses of all structural nodes subjected to different seismic combinations while the concentrated damping characteristic exists within internal parts of structure based on four seismic calculation models. **a** Seismic combination [A, A], **b** Seismic combination [A, B], **c** Seismic combination [A, C], **d** Seismic combination [A, D]

results obtained with the acceleration model for the different seismic combinations. Because error produced by the acceleration model usually appear at internal parts of the structure, only internal parts are addressed here. Figure 18 shows that under uniform earthquake excitation the acceleration model can be considered accurate. Increases in the difference in earthquake excitations at two supports correspond to increasing errors produced by the acceleration

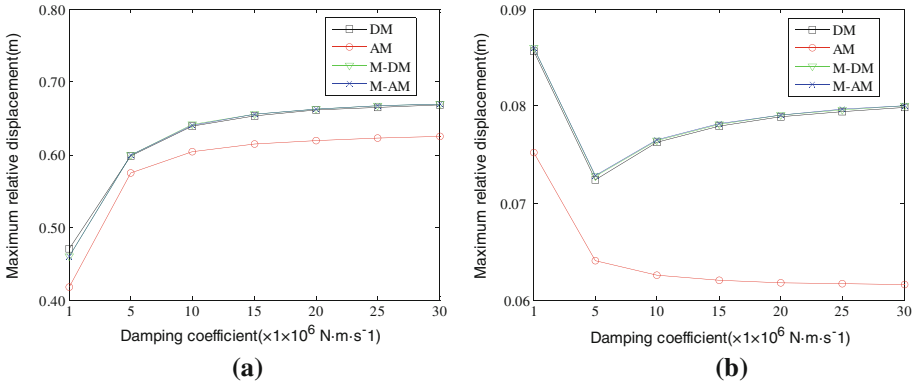

Fig. 19 Maximum displacement responses of node 1 and 4 corresponding to different damping coefficients based on four seismic calculation models. **a** Node 1. **b** Node 4

model. This is mainly because $(\boldsymbol{C}_{\mathrm{sb}} + \boldsymbol{C}_{\mathrm{s}}\boldsymbol{\Gamma}_{sb})$ in the ignored term, $-(\boldsymbol{C}_{\mathrm{sb}} + \boldsymbol{C}_{\mathrm{s}}\boldsymbol{\Gamma}_{sb})\,\dot{\boldsymbol{U}}_{\mathrm{b}}$ of the acceleration model, there is a two-column matrix, and elements in the first and second columns corresponding to concentrated damping are usually of similar size and opposite in sign. Only when each earthquake excitation in $\dot{\boldsymbol{U}}_{\mathrm{b}}$ is different may the ignored term play a key role and lead to some obvious error with the acceleration model. The greater the difference of earthquake excitations between two supports, the greater the error of the acceleration model. Therefore, it can be concluded that different earthquake inputs at supports influence the accuracy of the acceleration model.

When dampers are installed within internal parts of the structure, concentrated damping exists in the positions where they are installed. In this next numerical analysis, the influence of the damping coefficient on calculation error with the acceleration model is studied. As in the previous analysis of concentrated damping at supports, we define constant value CD=$1\times10^6\ \mathrm{N}\times\mathrm{m}\times\mathrm{s}^{-1}$ and adopt four damping coefficient values, $\mathrm{c_d} = [1, 5, 10, 20]\times\mathrm{CD}$. Seismic combination [A, D] is used as input. Two representative nodes, 1 and 4, are selected, and displacements of the two nodes relative to nodes 0 and 5, respectively, are used as research indices. Figure 19 illustrates the change in the maximum response values of node 1 and 4 with variation in the damping coefficient. For node 1, when the damping coefficient increases, the response calculated with the acceleration model first decreases and then becomes stable. For node 4, when the damping coefficient increases, the response first increases and then becomes stable. The error change associated with the acceleration model for different damping coefficients can be described by error indices ρ_{DM} and ρ_{AM} in Eq. (32). Adopting damper configuration 3, Fig. 20 describes error situations of relative displacement responses of structural nodes calculated by the acceleration model. Different error magnitudes are observed to exist in the displacement responses of the different structural nodes calculated by the acceleration model. These errors tend to be stable despite increases in the damping coefficient, as illustrated by Fig. 21 for damper configuration 4.

6 Conclusions

This paper presents a systematic study of calculation models for seismic analysis of long-span structures under multi-point excitation in an earthquake. Several calculation models are derived based on dynamic theory, and then an important but often overlooked problem in

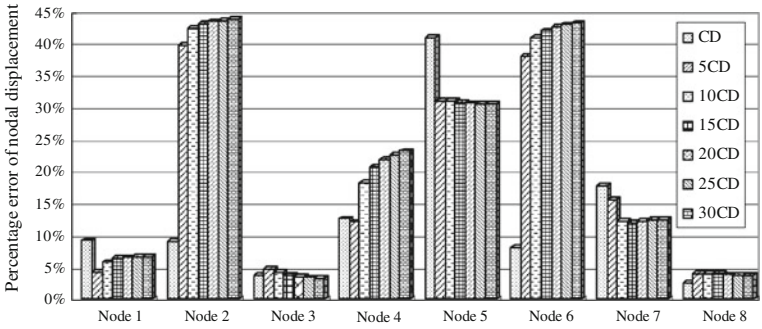

Fig. 20 Error of calculation responses of all structural nodes corresponding to different damping coefficients in damper configuration 3 based on acceleration model

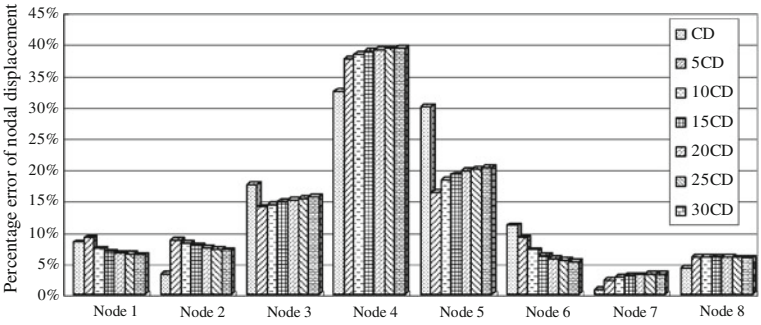

Fig. 21 Error of calculation responses of all structural nodes corresponding to different damping coefficients in damper configuration 4 based on acceleration model

conventional calculation models is identified and described. Sources of error and situations in which they may occur with the displacement model and the acceleration model are explained, and model modifications for time history and stochastic analysis are presented. Based on the theoretical derivations and numerical analyses presented in this paper, the following conclusions are drawn:

(1) The displacement model and the acceleration model have different ranges of applicability in seismic analysis of long-span structures. The displacement model is applicable for both linear and nonlinear analysis, but the acceleration model can only used in linear cases because of the adoption of the superposition principle in its derivation. The errors of the two models are both produced by ignoring the damping terms, such that the error problem is actually a damping problem. It should be noted that the two models have different damping assumptions and error-induced mechanisms.
(2) For an ordinary structure with Rayleigh damping, the displacement model is sufficiently accurate for calculation of the seismic response structure, except when the bottom elements are too finely divided. Obvious errors occur mainly in the calculated displacements of bottom elements and are affected by elemental division. For structures with dampers at the bottom, both damping coefficients provided by dampers and the ratio of ground velocity to acceleration (PGV/PGA) have an important influence on the magnitude of error associated with the displacement model, so that in a near-fault earthquake, the error is more obvious. Unlike the case with an ordinary structure, errors occur for both the

bottom and internal parts of long-span structure. Increases in the damping coefficient correspond to increasingly obvious errors for bottom elements, while errors for internal elements tend to remain stable.

(3) In an ordinary structure with Rayleigh damping, the acceleration model has good calculation precision and is not influenced by bottom elemental division, so it can be considered an accurate method of seismic analysis for this type of structure. When dampers are installed in the structure, regardless of whether concentrated damping exists at the bottom or within internal parts of the structure, the calculation precision of the acceleration model will be affected, and some error will result.

(4) When concentrated damping exists at the supports, the responses of all structural nodes calculated with the acceleration model exhibit obvious error. As with the displacement model, the error of the acceleration model is mainly a function of the damping coefficients and the ratio of ground velocity to acceleration (PGV/PGA), so there is obvious error in the calculated accelerations in the case of a near-fault earthquake. Increases in the damping coefficient correspond to increasingly obvious errors for bottom elements, while errors for internal elements tend to remain stable.

(5) When concentrated damping exists within the internal parts of the structure, the error produced by the acceleration model for bottom elements is relatively small, and some error is also produced for the internal parts. Similarly, the error produced by the acceleration model is affected by the damping coefficient and the ratio of ground velocity to acceleration (PGV/PGA), so there is obvious error in the calculated accelerations in the case of a near-fault earthquake. Errors produced by the acceleration model are closely related to the damper configurations and the different motions of multiple supports in an earthquake. Increases in the damping coefficient correspond to increasingly obvious errors for the bottom elements, while errors for internal elements tend to remain stable. Differences in the motion of all of the supports in an earthquake affect the error associated with the acceleration model, and while the differences tend to be distinct, the errors tend to be obvious. If there are no differences in the motion of the supports, the error produced by the acceleration model is too small to be neglected.

(6) The modification to the time history analysis method described in this paper based on fundamental dynamic theory and yields results equal in accuracy to those obtained by the large mass method or the large stiffness method. Moreover, based on the pseudo-excitation method, stochastic expressions are derived and improved to conduct efficient and accurate calculations. Given that the pseudo-excitation method utilizes random excitation as a sinusoidal input, the calculation error associated with stochastic analysis is similar in magnitude to that associated with time history analysis.

Acknowledgements The National Natural Science Foundation of China (No.50938008, 51108466), the National Science Foundation for Post-doctoral Scientists of China (No.20110491277), the Science Foundation for Post-doctoral Scientists of Central South University, the Freedom Explore Program of Central South University, the Scientific Research Foundation of Central South University.

References

Berrah M, Kausel E (1993) A modal combination rule for spatially varying seismic motions. Earthq Eng Struct Dyn 22(9):791–800

Clough RW, Penzien J (1975) Dynamics of structures. McGraw-Hill Book Co, New York

Hao H (1991) Response of multiply-supported rigid plate to spatially correlated seismic excitations. Earthq Eng Struct Dyn 20(9):821–838

Hao H, Xiao ND (1995) Response of asymmetric structures to multiple ground motions. J Struct Eng 121(11):1557–1564

Kiureghian AD, Ansgar N (1992) Response spectrum method for multi-support seismic excitations. Earthq Eng Struct Dyn 21(8):713–740

Lin JH (1992) A fast CQC algorithm of PSD matrices for random seismic responses. Comput Struct 44(3):683–687

Liu GH, Guo W, Li HN (2010) An effective and practical method for solving an unnegligible problem inherent in the current calculation model for multi-support seismic analysis of structures. Sci China (Technological Sciences) 53(7):1774–1784

Su L, Dong SL, Kato S (2006) A new average response spectrum method for linear response analysis of structures to spatial earthquake ground motions. Eng Struct 28(13):1835–1842

Wilson EL (2004) Static and dynamic analysis of structures: a physical approach with emphasis on earthquake engineering. Computer and structures, Inc., Berkley

Yamamura N, Tanaka H (1990) Response analysis of flexible MDF systems for multiple-support seismic excitation. Earthq Eng Struct Dyn 19(3):345–357